Wear 320 (2014) 161–178

Contents lists available at ScienceDirect

Wear

journal homepage: www.elsevier.com/locate/wear

Boundary lubrication: Influence of the size and structure of inorganic fullerene-like MoS_2 nanoparticles on friction and wear reduction

Pierre Rabaso [a,b,c,*], Fabrice Ville [a], Fabrice Dassenoy [b], Moussa Diaby [c], Pavel Afanasiev [d], Jérôme Cavoret [a], Béatrice Vacher [b], Thierry Le Mogne [b]

[a] Université de Lyon, LaMCoS, UMR CNRS 5259, INSA de Lyon, 18–20 Rue des Sciences, F69621 Villeurbanne Cedex, France
[b] Université de Lyon, LTDS, UMR CNRS 5513, Ecole Centrale de Lyon, 36 Avenue Guy de Collongue, F69134 Ecully Cedex, France
[c] PSA Peugeot Citroën Centre Technique de Belchamp, France
[d] Université de Lyon, IRCELYON, UMR CNRS 5256, 2 Avenue Albert Einstein, F69626 Villeurbanne Cedex, France

ARTICLE INFO

Article history:
Received 2 June 2014
Received in revised form
29 August 2014
Accepted 2 September 2014
Available online 21 September 2014

Keywords:
Solid lubricants
Lubricant additives
Boundary lubrication
Nanotribology
IF-MoS2 nanoparticles

ABSTRACT

The use of Inorganic Fullerene-like (IF) nanoparticles in lubricants has proved extremely effective to reduce friction and wear under severe boundary lubrication conditions. It has furthermore been suggested that the synthesis of smaller nanoparticles containing many structural defects would benefit friction and wear reduction, as they would penetrate and exfoliate more easily in the contact, leading to the quick formation of homogeneous tribofilms. In this study, four different types of IF-MoS_2 were synthesized so as to be able to differentiate the influence of both the size and the morphology of the nanoparticles on their tribological behavior. Pure-sliding, reciprocating tribological testing of these four types of nanoparticles revealed their excellent friction-reducing properties in severe boundary lubrication, with splash lubrication taking place for a high number of cycles. High wear reduction was also obtained and confirmed using optical profilometry. Although the nanoparticle structure was found to have an influence on their effectiveness in time, all the nanoparticles tested – regardless of size or crystallinity – were found to achieve the same performances as long as proper oil recirculation took place, ensuring a continuous feeding of the contact in nanoparticles. The formation of MoS_2 tribofilms on the wear surfaces was confirmed using XPS analyses and observed on FIB cross sections, and their nature was discussed in the light of the associated tribological results. As the size and morphology of the IF-MoS_2 did not affect their performance in the range studied, their friction reducing properties were compared to those of bulk h-MoS_2 tested in the same conditions. The benefits of using spherical nanoparticles such as IF-MoS_2 was clearly shown.

© 2014 Elsevier B.V. All rights reserved.

1. Introduction

The use of nanoparticles as lubricant additives has been widely explored in recent years, and the advances in synthesis techniques [1–3] have revealed the tribological potential of many different types of nanoparticles. Nanospheres and nanotubes (or nanowires) of different nature have been studied, such as for example carbon nano-onions [4], cobalt-based carbon nanotubes [5], $Mo_6S_3I_6$ nanowires [6] or more recently combinations of iron, copper, and cobalt nanoparticles [7]. Inorganic fullerene-like disulfide nanoparticles, and more specifically IF-MoS_2 and IF-WS_2, have however generated a special interest due to their very low friction and wear reduction properties in severe boundary lubrication regimes [8–11]. Different lubrication mechanisms thought to be associated with these nanoparticles have been described in the literature. First proposed by Cizaire et al. [8] in the case of IF-MoS_2, the exfoliation of IF-WS_2 nanoparticles submitted to high contact pressures into several nanosheets was later observed by Joly-Pottuz et al. [12]. This was confirmed by in situ TEM imaging of IF-MoS_2 nanoparticles under different shear and compression conditions [13,14]. The nanoparticles undergo a rolling process for sliding conditions under low contact pressures, whereas they suffer large deformations and then exfoliation of the outer sheets for higher contact pressures (around 1 GPa). The behavior of IF-WS_2 was found to be quite similar, and the extent of their elastic deformation was successfully observed using HRSEM and used to give an estimation of the compression failure strength of nanoparticles of different sizes and shapes [15]. The three prominent friction mechanisms associated to individual multilayered nanoparticles were then summed up by the same authors and verified experimentally using in situ HRSEM [16], namely (a) rolling for

* Corresponding author at: LaMCoS (INSA Lyon) – LTDS (Ecole Centrale de Lyon) – PSA Peugeot Citroën, INSA Lyon, 18-20, rue des Sciences, 69100 Villeurbanne, France. Tel.: +334 72 43 70 81.
E-mail address: pierre.rabaso@insa-lyon.fr (P. Rabaso).

http://dx.doi.org/10.1016/j.wear.2014.09.001
0043-1648/© 2014 Elsevier B.V. All rights reserved.

low shear rates and relatively low normal stresses (0.96 ± 0.38 GPa), (b) sliding for slightly higher normal stresses and (c) exfoliation for high normal stresses (above 1.2 GPa).

The relationship between this exfoliation process under high contact pressures and the considerable performances of fullerene-like nanoparticles in boundary lubrication regimes was further investigated in [17], where the friction reduction was shown to originate from the adhesion of a tribofilm composed of the resulting hexagonal 2H-MoS_2 nanosheets on the steel surfaces. The crystallinity of the nanoparticles was also shown to be of great influence on their friction reduction capacities, as the presence of many defects will facilitate the exfoliation mechanism, enabling a faster tribofilm formation on the contacting surfaces [18].

According to the literature, and considering the exfoliation mechanism taking place in the boundary lubrication regime, the general agreement today is that the synthesis of smaller fullerene-like nanoparticles will improve friction reduction, by increasing the probability of the nanoparticles passing through the contact. To the author's knowledge, this remains an assumption as no study has yet compared the tribological performances of similar IF-MoS_2 varying only in size. Small nanoparticles however generally show interesting results, such as the poorly crystalline nanoparticles tested in [18] for example, with a diameter comprised between 20 and 50 nm. The larger and less efficient IF-MoS_2 nanoparticles tested in the same operating conditions were however also more crystalline, which makes it difficult to conclude on the influence of nanoparticle size alone. The benefits in reducing the size of IF-WS_2 aggregates has furthermore been shown, either by an effective mixing of the oil before testing [19,20] or by grafting the appropriate dispersants on the nanoparticles [21].

In this study, the tribological behavior of four types of IF-MoS_2 nanoparticles of different sizes and degrees of crystallinity was explored, by comparing their friction and wear reduction capacities under severe boundary lubrication regimes. The results obtained during these tests made it possible to differentiate the influences of nanoparticle size and crystallinity.

2. Experimental

2.1. Tribological tests

All the tribological tests showed in this article were carried out on a PCS Instruments HFRR (High Frequency Reciprocating Rig). The test consists in a pure-sliding reciprocating motion between a diameter 6 mm ball and a flat, with a maximum contact pressure of 1.4 GPa. The test is schematized and the conditions are given on Fig. 1. The contact pressure and the very low surface separation are typical of the severe boundary lubrication met in automotive applications, such as gears or the valve train.

The base oil was the same for all the IF-MoS_2 nanoparticles tested in this study, a blend of PAO 4 and PAO 40, with a viscosity of 9.3 cSt at 100 °C and 54.0 cSt at 40 °C. The materials used were polished AISI 52100 (100Cr6) steel ($Ra < 50$ nm for the ball and $Ra < 20$ nm for the flat). All the tests were carried out for an identical mass concentration of IF-MoS_2. This concentration was arbitrarily set to 1 wt% for the purposes of this study, as it relates to many studies already published and was shown to be optimal for similar applications in the literature [8–11,17,18,20]. The oil was thoroughly mixed using a magnetic agitator, and the 2 mL test sample was then placed in the HFRR lower specimen holder immediately before the beginning of the test. The authors deliberately chose not to use an ultrasonic bath for the mixing, so as to obtain a dispersion representative of real-life test conditions. The high number of cycles achieved during the test (144 000) was chosen to provide information on the different nanoparticles' capacity to maintain their tribological performances in time.

All the HFRR test results presented in this article were repeatable, and a single, typical graph is presented as a result for each test for the sake of clarity.

2.2. Observation and characterization

The topography of the wear scars on the flat counter-surface was obtained using an optical Sensofar PLu neox profilometer, providing information on their depth, volume, length and width. The choice of analyzing the flat surface instead of the ball was made so as to reveal if any plastic deformation took place during the test. The criteria chosen to quantify the wear were the maximum depth of the scar, and the volume of steel lost during the test. This worn volume was obtained by subtracting the plastically deformed matter (total volume above the mean surface) to the volume of the scar (total volume below the mean surface).

A JEOL 2010F operating with 200 kV accelerating voltage was used for the TEM observations of the nanoparticles. To achieve this, a drop of highly diluted IF-MoS_2 in heptane was deposited onto a standard carbon-covered-copper microgrid. In order to fully characterize the tribofilm formed on the flat, TEM samples were prepared using the FIB technique. A transversal cut was performed on the worn surface to obtain a 100 nm thick cross section. Platinum and tungsten layers were previously deposited on the worn track to preserve the surface from nanomachining by $Ga+$ ion beam.

Chemical analysis of the tribofilms was performed by XPS. With a probing depth of a few nanometers (5 nm), this technique is the most convenient for surface analysis and wear scar characterization. An Ulvac-PHI Versaprobe II system, with a high power monochromatized Al K_α X-ray source ($hv = 1486.68$ eV), was used. The X-ray beam was focused in the wear scar and an area of 100×100 μm was probed. A survey scan was first recorded in order to identify the chemical elements present in the probed area. Scans were then recorded at some selected peaks in order to get complete information on the chemical composition (chemical bonding) of the tribofilm. The resolution of the XPS was 0.2 eV, and the position of C 1s peak (284.8 eV) was considered as the reference for charge correction. A flood gun was used for charge compensation. The XPS analyses were performed in several areas, in order to verify the repeatability of the results. Multi Pack software was used to analyze the XPS spectra obtained from long scans. Quantitative analyses of the peaks were performed using

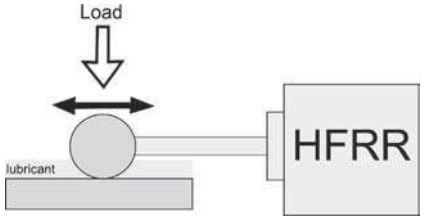

Load (N)	10
Maximum hertzian pressure (GPa)	1.4
Stroke length (mm)	1
Frequency (Hz)	10
Cycles	144 000
Oil capacity (mL)	2
IF-MoS_2 concentration (wt%)	1
Temperature (°C)	80

Fig. 1. Schematic of the HFRR and conditions used for the tribological tests.

peak area sensitivity factors. A XPS handbook and online databases were used to attribute the binding energies to chemical species.

2.3. Nanoparticle synthesis

All the nanoparticles presented in this study were synthesized at IRCELYON. The synthesis is a two-step process. The first step was the preparation of nanoparticles of amorphous MoS_x ($x > 3$) compound by chemical reaction of ammonium heptamolybdate and sulfur in ethylene glycol under reflux. The process was similar to the preparation described in [22] but instead of cellulose, an equivalent amount of amidon was added to the reaction mixture. The reaction conditions were modified to obtain particles of different size, by changing the order of addition of the reactants, the duration and the temperature. Thus to obtain large particles, the reactants were added simultaneously and then the mixture was heated for 4 h at the boiling point of ethylene glycol. To obtain smaller particles the solution of ammonium heptamolybdate was added subsequently in four equal portions with an interval of 5 min and then the reaction mixture was heated only for 1 h at 180 °C. After the reaction, the mixture was cooled to room temperature and diluted by a twofold excess of ethanol. The amorphous compound was then extracted by centrifugation, washed and dried. The second step consisted of treating the MoS_x powder in a quartz reactor under a flow of hydrogen and H_2S mixture. The thermal treatment step results in the formation of crystalline MoS_2 and eventually of the IF-MoS_2 nanoparticles. The second step may be carried out at different temperatures, lower temperatures leading to the formation of less crystallized nanoparticles, containing more structural defects. An overview of the characteristics of the four types of IF-MoS_2 synthesized is given in Table 1.

3. Results and discussion

3.1. High-resolution observation of the IF-MoS_2 nanoparticles

The four types of nanoparticles described in Table 1 were observed using HRTEM, and a narrow particle size distribution was noted (see Fig. 2).

The rather large size (300–400 nm) of the LpC and LC particles was confirmed, and their good sphericity was revealed (Fig. 3). The high-temperature (700 °C) thermal treatment carried out at the end of the synthesis process of the LC IF-MoS_2 improved the fullerene-like aspect of the structure, which is composed of long and concentric atomic layers. Some defects can however be observed in the nanoparticle structure, with some discontinuities between the layers. The lower temperature (400 °C) used for the thermal treatment of the LpC nanoparticle resulted in short MoS_2 layers (4–6 nm in length), stacked in a seemingly chaotic manner. Therefore, the particles treated at 400 °C do not have a fullerene-like aspect, and may be considered as spherical and poorly crystalline MoS_2 nanoparticles.

Table 1
Main characteristics of the first four types of IF-MoS2 nanoparticles synthesized.

Designation	Average diameter (nm)	Treatment temperature (°C)
LpC (Large, Poorly Crystalline)	350	400
LC (Large Crystalline)	350	700
SpC (Small, Poorly Crystalline)	150	400
SC (Small Crystalline)	150	700

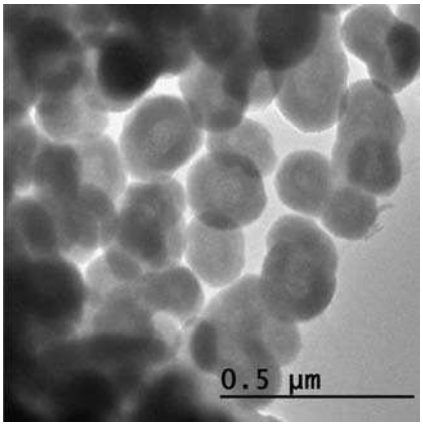

Fig. 2. Typical size distribution of the nanoparticles (SC IF-MoS_2 shown here).

The differences between the smaller SC and SpC nanoparticles are similar to those between the previous LC and LpC nanoparticles, with long and concentric atomic layers clearly visible in the first case and short and randomly stacked atomic layers in the other (Fig. 4). The term "IF-MoS_2" will however still include the LpC and SpC particles throughout this study, for the sake of simplicity.

The average diameter of the SC and SpC nanoparticles observed was approximately 150 nm, representing an average reduction by 2.33 compared to the LC and LpC IF-MoS_2. Considering perfectly spherical nanoparticles, this would imply a reduction by 12.65 in terms of volume. Since the nanoparticle concentration is constant in terms of mass, and assuming that all the nanoparticles in the study have the same density, this reduction in size also implies that the average number of SpC and SC nanoparticles in a given volume of oil is approximately 12.65 more than that of LpC and LC nanoparticles. This size reduction may affect not only the properties of single nanoparticles, but also their agglomeration and their availability throughout the oil medium.

The chemical composition of the IF-MoS_2 was verified using X-Ray Photoelectron Spectroscopy. The molybdenum (Mo 3d) and sulfur (S 2p) energy peaks for the four types of nanoparticles are shown in Figs. 5 and 6, respectively.

The main Mo $3d_{5/2}$ and S $2p_{3/2}$ peaks have the same energies for all four types of IF-MoS_2, confirming that they are of identical nature (Table 2). The Mo $3d_{5/2}$ peaks are found at approximately 229.8 eV and the S $2p_{3/2}$ at 162.7 eV, which are typical energy peaks corresponding to molybdenum sulfide species.

The surface of the LC and SpC nanoparticles appeared to be somewhat oxidized, with Mo – O species found at 232.5 eV and 233.9 eV for the LC IF-MoS_2 and 234.4 eV for the SpC IF-MoS_2. This was confirmed with the observation of S – O species at 169.1 eV and 170.3 eV (LC IF-MoS_2), and 168.7 eV and 170.7 eV (SpC). Partial oxidation of the surface may have occurred due to air exposure before the XPS experiments. This did however not appear to be due to the nanoparticle synthesis process or to the many defects in the nanoparticles (structure not as well closed), as both the LC and SpC were found to be oxidized but not the LpC and SC nanoparticles.

Small energy contributions were finally found at 164.1 eV (SpC) and 163.8 eV (LpC), which were attributed to a small excess of sulfur in the poorly crystalline nanoparticles.

3.2. Tribological testing of the four types of IF-MoS_2 nanoparticles

Fig. 7 shows the evolution of the friction coefficient for the large (LpC and LC) IF-MoS_2 nanoparticles during the 4 h HFRR test (operating conditions given in Fig. 1).

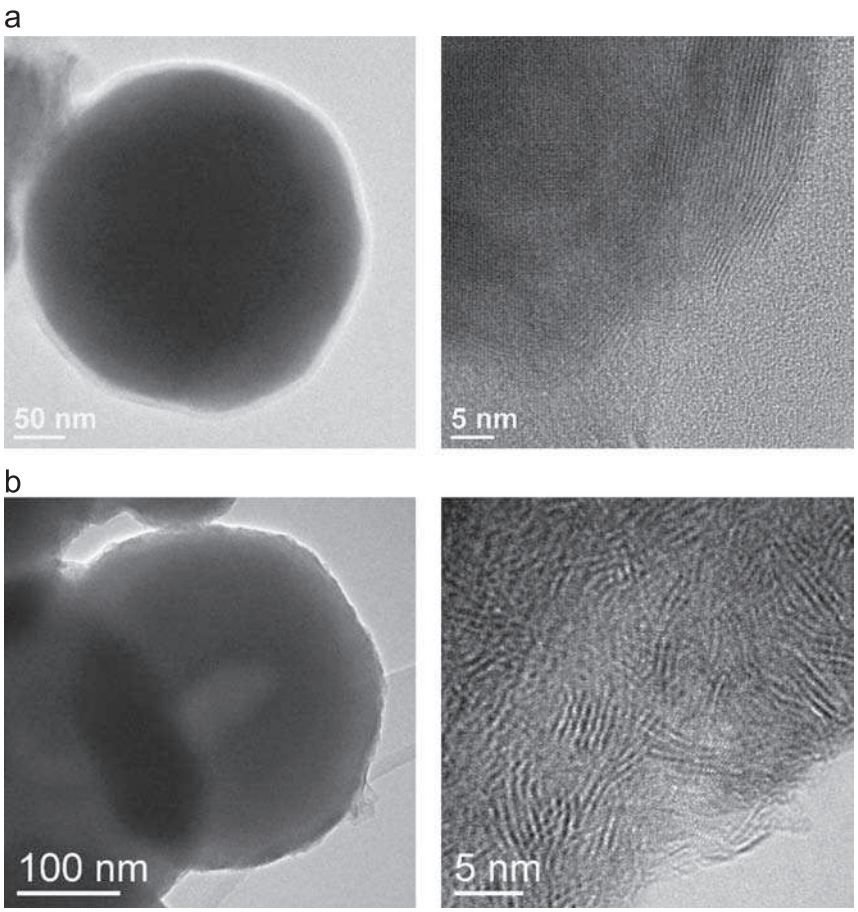

Fig. 3. HR TEM images of LC (a) and LpC (b) IF-MoS_2 nanoparticles.

Under these severe operating conditions, the reference test for the PAO oil produced a fairly constant friction coefficient of 0.2. Both types of large nanoparticles showed great friction reduction abilities, with a friction coefficient quickly dropping to 0.06. The LpC and LC nanoparticles showed similar behaviors at the beginning of the test, with the associated friction coefficient decreasing progressively before reaching minimum friction and stabilizing during approximately 75 000 cycles. The test results then differed, as the friction coefficient remained stable throughout the 144 000 cycles for the LpC IF-MoS_2-doped base oil, but started increasing continuously for the LC nanoparticle-doped PAO. The sudden raise in the coefficient of friction observed after approximately 85 000 cycles may be due to a progressive wearing out of the tribofilm formed on the friction surfaces, slowly increasing the coefficient of friction back to the value obtained for the base oil only.

The smaller SC and SpC IF-MoS_2 nanoparticles were tested with the same operating conditions, and the results are shown in Fig. 8.

The tribological behavior of these smaller SC and SpC nanoparticles was strikingly similar to that of the LC and LpC nanoparticles tested before. Both types of IF-MoS_2 decreased the friction coefficient abruptly at the beginning of the test, which then stabilized between 0.06 and 0.07. While the small and poorly crystalline SpC nanoparticles maintained the friction coefficient stable throughout the 144 000 cycles of the test, the more crystalline IF-MoS_2 were once again effective only for a limited number of cycles, as the friction coefficient started increasing after 85 000 cycles until it reached the value obtained for the base oil alone.

The extreme friction reduction abilities of IF-MoS_2 nanoparticles in severe boundary lubrication regimes have been shown before [8,10,17,18], but for fairly mild test conditions: ambient temperature, low number of cycles (under 2000) and a deposition of one or two droplets of the formulated oil on the specimen at the beginning of the test. The test results depicted in Figs. 7 and 8 highlight the efficiency of IF-MoS_2 nanoparticles under conditions more likely to be encountered in real-life applications, with a high number of cycles achieved and splash lubrication taking place in a small volume of oil. All four nanoparticle types proved to be very effective additives, by reducing friction by approximately 70% compared to the base oil alone for a high number of cycles (75 000 cycles of maximum friction reduction for the least durable type of IF-MoS_2).

When comparing the tribological results for both sets of nanoparticles (large and small), it becomes clear that their crystallinity is the main parameter dictating their effectiveness, predominant over particle size (Fig. 9). Both types of poorly crystalline nanoparticles (large and small) indeed produced a very low friction coefficient throughout the whole test, whereas both types of more crystalline IF-MoS_2 (large and small) were only effective until 85 000 cycles were reached. For these LC and SC nanoparticles, the friction coefficient then rose steadily throughout the test before reaching the value obtained for the base oil alone, behavior attributed to the progressive wearing out of the tribofilm.

As a complement to the friction coefficients recorded for the LC, LpC, SC and SpC nanoparticle types, the corresponding wear scars were compared. The corresponding quantities (the maximum scar depth measured, the measured scar volume, the measured volume of deformed matter and the calculated worn volume) are reported in Table 3. For the sake of clarity, the criteria chosen to quantify the wear were also plotted on Fig. 10.

In addition to their friction-reducing properties, the IF-MoS_2 nanoparticles have reduced wear significantly during the tests.

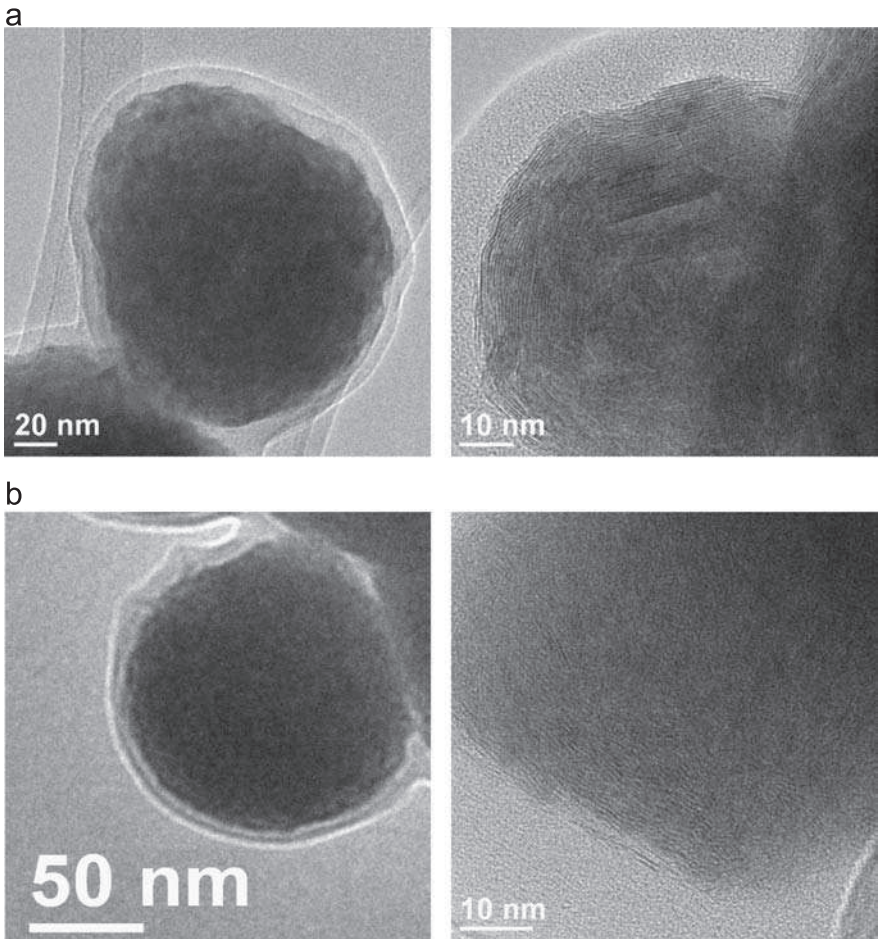

Fig. 4. HR TEM images of SC (a) and SpC (b) IF-MoS_2 nanoparticles.

Both types of poorly crystalline particles (large and small) were more effective in reducing wear than the more crystalline IF-MoS_2, which is consistent with the friction results showed previously.

3.3. *Effects of the oil flow in nanoparticle starvation of the contact*

For the nanoparticle sizes and morphologies studied, the crystallinity did not have a significant influence on the minimum friction coefficient achieved, but it had a great impact on the durability of the additive during the test. As the mass concentration was the same for all four samples (1 wt%) but only the poorly crystalline IF-MoS_2 (both small and large) proved durable, the shorter effectiveness of the SC and LC nanoparticles is not likely to be due to a full consumption of all the IF-MoS_2 in the oil sample after 85 000 cycles. The number of nanoparticles was indeed theoretically similar for the LC and LpC samples on the one hand and for the SC and SpC samples on the other, meaning that the rate at which they pass through the contact should be comparable. The poorly crystalline LpC and SpC nanoparticles being in theory less resistant to the combined solicitations of normal pressure and shear [13,14,18], their consumption should be faster than that of crystalline IF-MoS_2 passing through the contact at the same rate.

In order to explain the shorter effectiveness of the LC and SC additives, a schematic top view of the HFRR setup is shown in Fig. 11. The reciprocating motion of the ball (upper specimen) on the flat (lower specimen) is thought to progressively draw the nanoparticles away from the contact, causing it to be starved in nanoparticles as the test goes on. This will slow down tribofilm formation, until it wears off faster than it regenerates. Friction then starts rising as the tribofilm wears off.

Considering that all IF-MoS_2 have the same density, it seems safe to assume that nanoparticles of same size will behave similarly when subjected to the oil flow during the HFRR test. The durability of the poorly crystalline nanoparticles, compared to the more crystalline ones (either large or small), indicates that fewer of these particles are needed to form and maintain the tribofilm on the specimen surface. This is consistent with their bigger ability to exfoliate under the combined efforts of normal pressure and shear reported in the literature.

In order to verify the hypothesis of a progressive nanoparticle starvation of the contact, another HFRR test was carried out on the LC sample (PAO+1 wt% LC) but with a higher frequency (20 Hz instead of the 10 Hz used before and reported on Fig. 1). The duration of the test was unchanged (4 h), which lead to a greater number of cycles than previously (288 000 instead of 144000). As the stroke remained the same, the average velocity of the ball on the disc was doubled, leading to milder contact conditions. In these conditions, the base oil alone produced a coefficient of friction averaging 0.19, while the addition of 1 wt% of LC permitted a minimum coefficient of friction of 0.07 (Fig. 12).

This lower efficiency in terms of friction reduction was predictable as fullerene-like nanoparticles are known to be most efficient for more severe lubrication regimes, their exfoliation (and thus tribofilm formation) being then facilitated [10]. The maximum friction reduction did however not last long, as the coefficient of friction started increasing progressively after only 1100 s (22 000 cycles). This result confirms that the nature of the test tends to progressively starve the contact in nanoparticles, phenomena which will occur faster if the frequency of the reciprocating motion is increased. The reducing number of nanoparticles

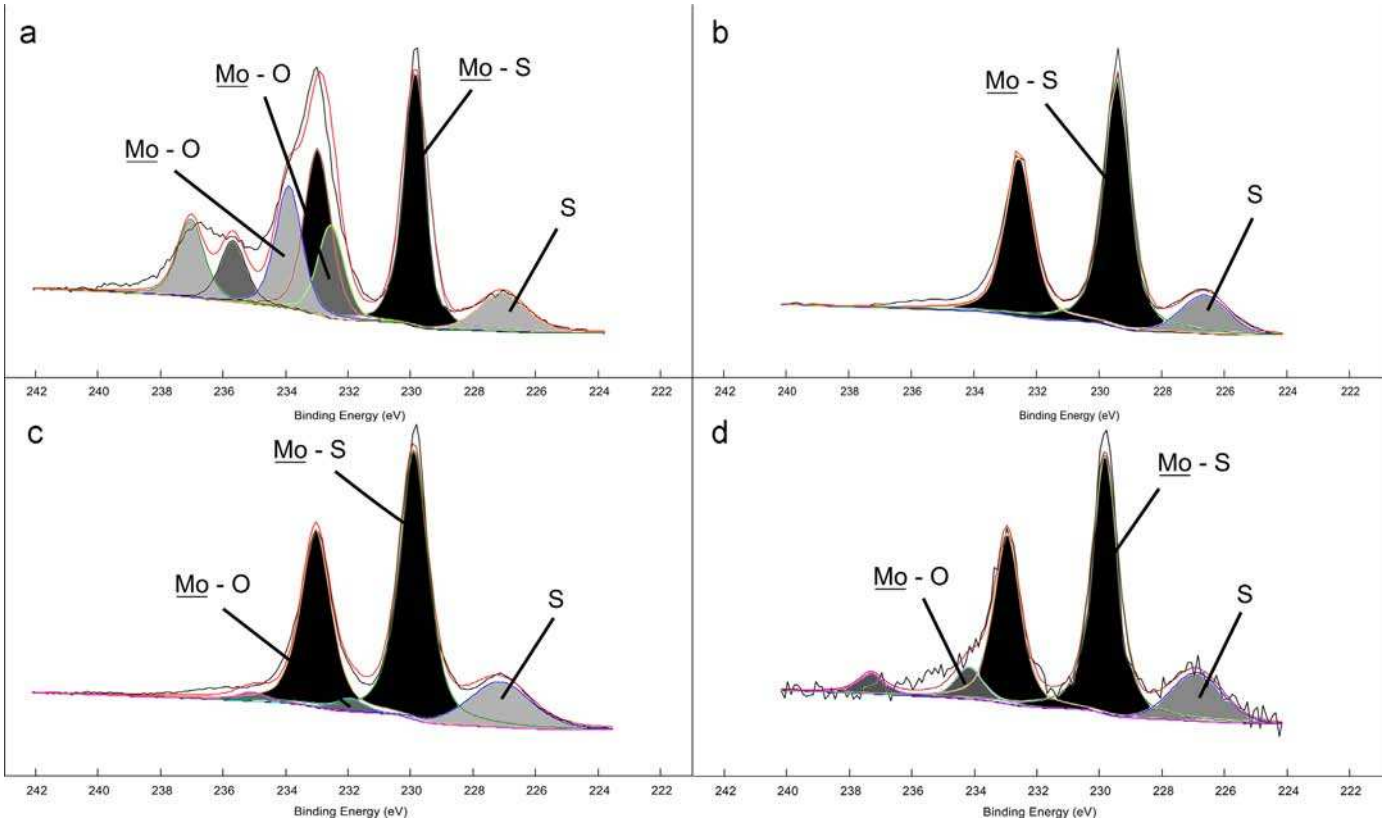

Fig. 5. Molybdenum 3d spectra measured by XPS for the (a) LC, (b) LpC, (c) SC and (d) SpC IF-MoS2.

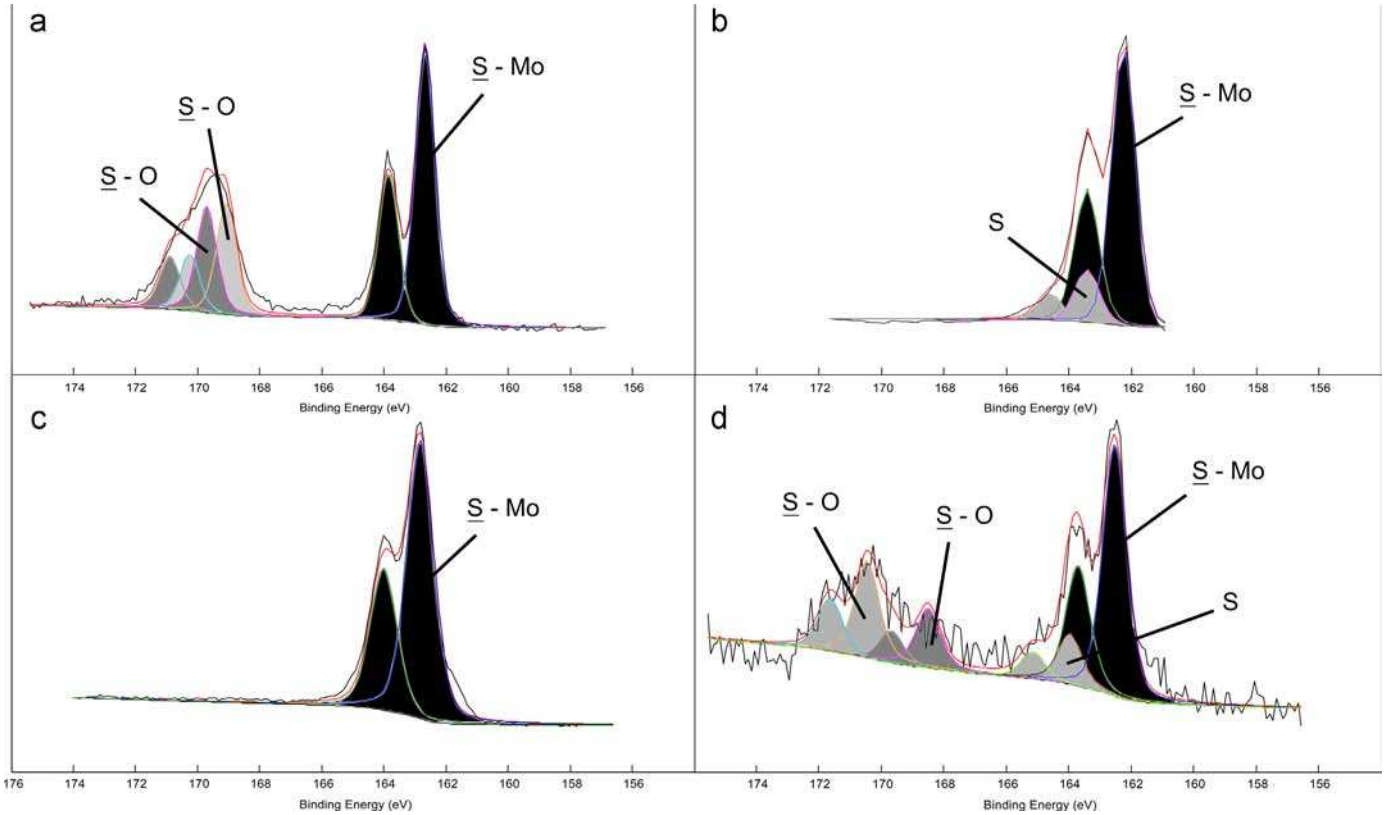

Fig. 6. Sulfur 2p spectra measured by XPS for the (a) LC, (b) LpC, (c) SC and (d) SpC IF-MoS2.

passing through the contact will slow down tribofilm regeneration until it is worn off or damaged, resulting in an increase in friction. In order to verify this hypothesis, this last HFRR test was repeated and interrupted after 17 min (1020 s), in order to compare the surface compositions during maximum friction reduction and at the end of the test (Fig. 13).

XPS analyses were carried out on these worn surfaces to confirm that the increase of friction was due to a deterioration of the tribofilm, reinforcing the hypothesis of a progressive starving of the contact in nanoparticles during the test. The results for the molybdenum (Mo 3d) and sulfur (S 2p) energy peaks are shown in Fig. 14. After 17 min of testing (top spectra), Mo $3d_{5/2}$ peaks corresponding to Mo – S species appear at 229.8 eV, which was also the energy peak of the MoS_2 found in the nanoparticles (see Table 2). The corresponding S $2p_{3/2}$ peak was found at 162.0 eV, confirming the presence of a MoS_2 tribofilm on the wear surface. The shifting of this peak towards the lower energies (from 162.7 eV for the LC IF-MoS_2 to 162.0) may indicate the presence of iron sulfides, and Mo – O species were also found at 232.2 eV. These S – Fe and Mo – O bonds are consistent with the presence of an MoS_2 tribofilm on an Fe substrate [17]. After the end of the four hour test, the very low intensities made it difficult to distinguish the Mo 3d and S 2p peaks (bottom spectra on Fig. 14). The atomic concentrations of iron compared to molybdenum and sulfur (Fe/(Fe+Mo+S) ratio) increased from 26 at.% after 17 min of testing to 68 at.% at the end of test, confirming the deterioration of the MoS_2 tribofilm.

Table 2
Measured energies for the main Mo and S peaks.

	Nanoparticle type			
	LC	**LpC**	**SC**	**SpC**
Mo $3d_{5/2}$	229.8 eV	229.8 eV	229.9 eV	229.8 eV
S $2p_{3/2}$	162.7 eV	162.6 eV	162.8 eV	162.7 eV
S 2s	227.0 eV	227.0 eV	227.1 eV	227.0 eV

These analyses confirm the formation of an MoS_2 tribofilm from the IF-MoS_2 at the beginning of the tribological tests. Due to the reciprocating nature of the HFRR, a progressive starvation of the contact in nanoparticles occurs during the tests, until the tribofilm can no longer regenerate and is progressively damaged, resulting in an increase in friction. The benefit in using less crystalline nanoparticles was then confirmed, as fewer are needed to maintain an effective tribofilm on the friction surfaces.

These tests showed that the efficiency of IF-MoS_2-induced friction reduction depends partly on the nature of the nanoparticle, but also of the oil flow around the contact. An additional test was carried out in order to verify if the performance of the less efficient LC nanoparticles could be enhanced by creating an artificial oil recirculation. This was achieved by stirring manually the oil in the bottom specimen holder of the HFRR with a clean steel rod during the first and third hour of the test. The result is shown in Fig. 15, where the friction coefficients are compared for

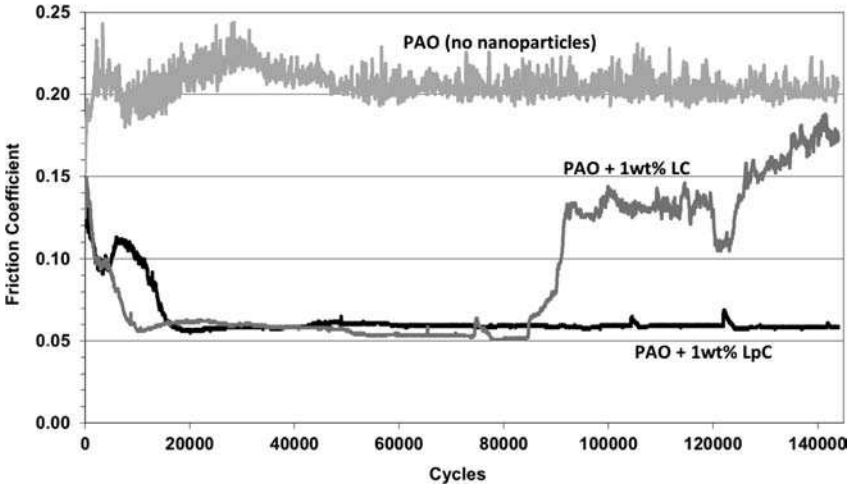

Fig. 7. Friction coefficients of the LC and LpC nanoparticles during the HFRR test.

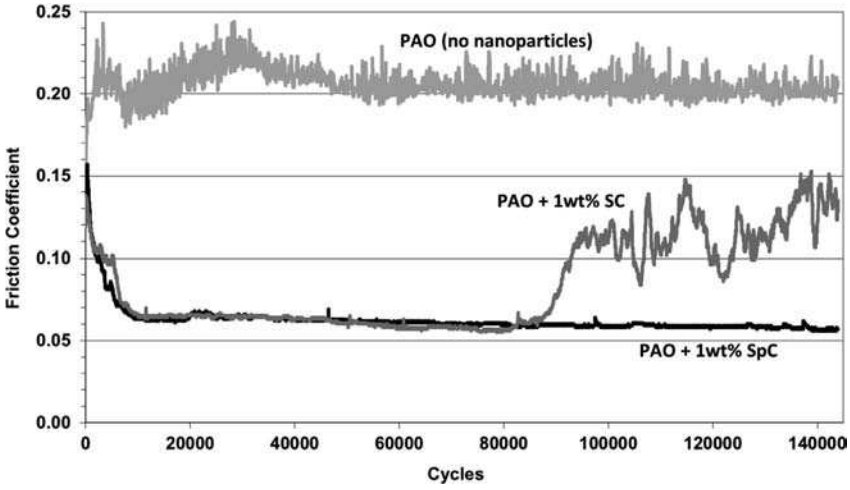

Fig. 8. Friction coefficients of the SC and SpC nanoparticles during the HFRR test.

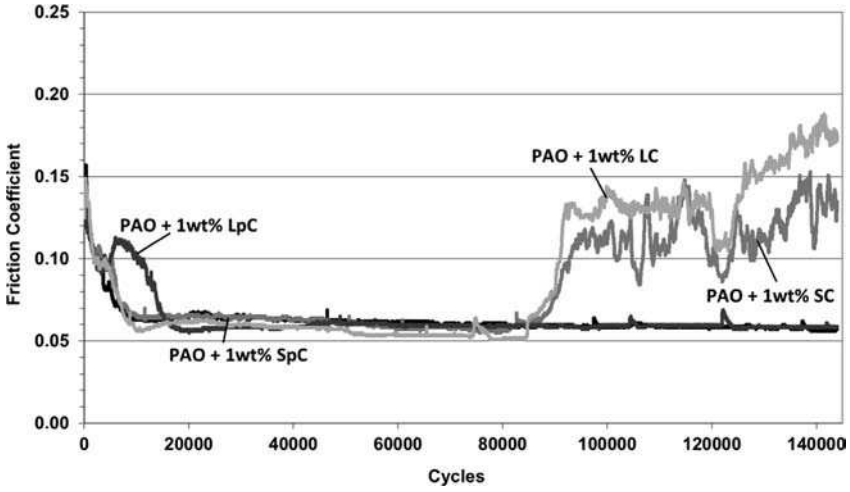

Fig. 9. Compared friction coefficients for the four types of nanoparticles tested.

Table 3
Depths and volumes of the wear scars obtained after tribological testing

Criteria test	Max. depth (μm)	Scar volume ($\times 10^3$ μm^3)	Deformed volume ($\times 10^3$ μm^3)	Worn volume ($\times 10^3$ μm^3)
No IF-MoS_2 (ref)	**13.6**	3 037	25	**3,012**
LC IF-MoS_2	**3.3**	254	43	**211**
LpC IF-MoS_2	**1.6**	136	43	**93**
SC IF-MoS_2	**2.5**	263	30	**233**
SpC IF-MoS_2	**1.2**	106	27	**79**

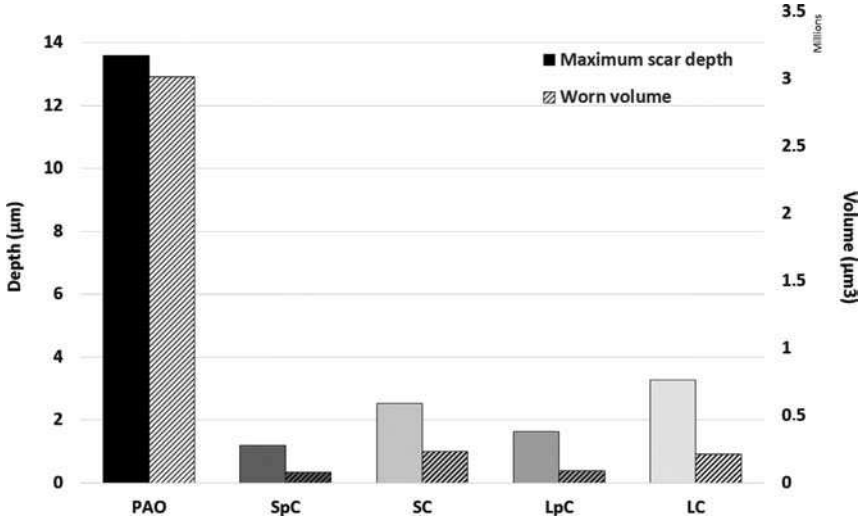

Fig. 10. Maximum depths and wear volumes of the scars obtained for the different types of IF-MoS2 tested.

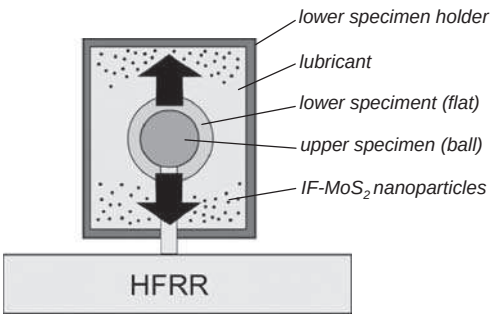

Fig. 11. Top view of the HFRR setup.

the stirred and unstirred LC-doped base oil. The manual stirring of the oil affected the measurement of the friction force, but a reference test carried out in the same conditions on the base oil alone showed that the average friction coefficient remained the same for the stirred and unstirred oil. During the first hour of the test, stirring the oil continuously stabilized the average friction coefficient to its lowest level, at 0.07. Recirculating the oil ensured a continuous feeding of the contact in nanoparticles, which is thought to have maintained a homogeneous tribofilm on the contact surfaces. When the stirring stopped after 72 000 cycles, the friction coefficient remained stable for approximately half an hour (36 000 cycles) before increasing drastically. This behavior is due to a wearing out of the tribofilm, due to a progressive

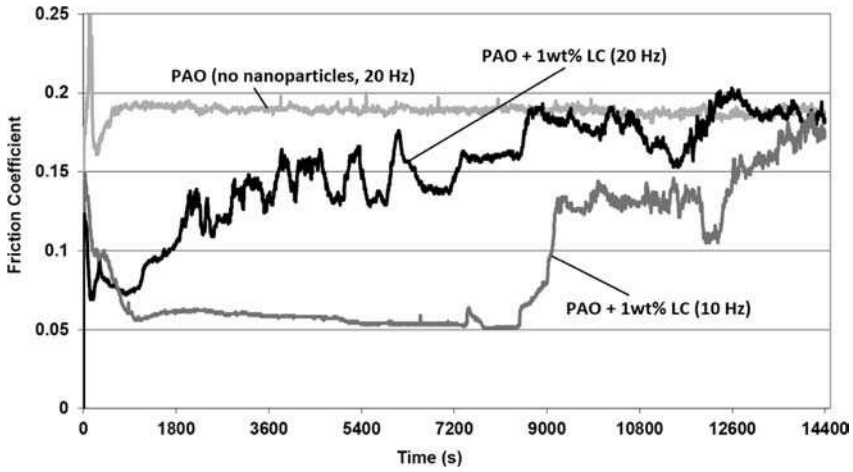

Fig. 12. Tribological behavior of LC nanoparticles for two operating conditions (10 Hz & 20 Hz).

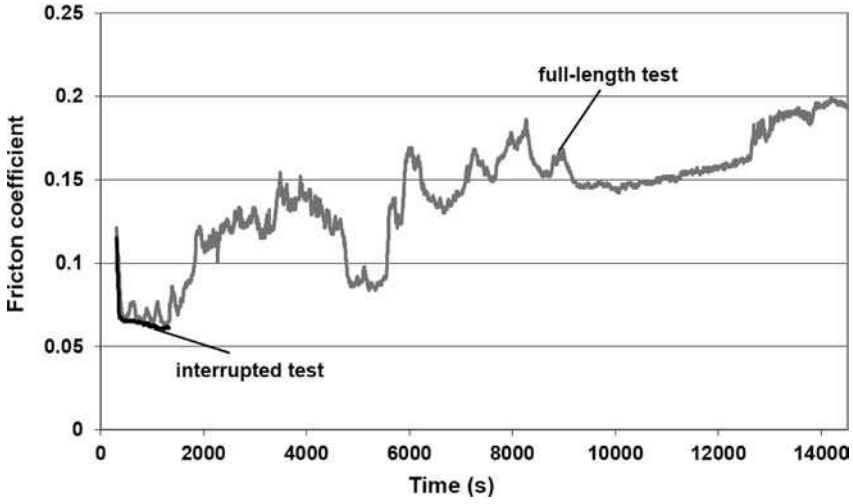

Fig. 13. Full-length and interrupted test using 1 wt% LC IF-MoS_2 in order to compare the surfaces during and after testing.

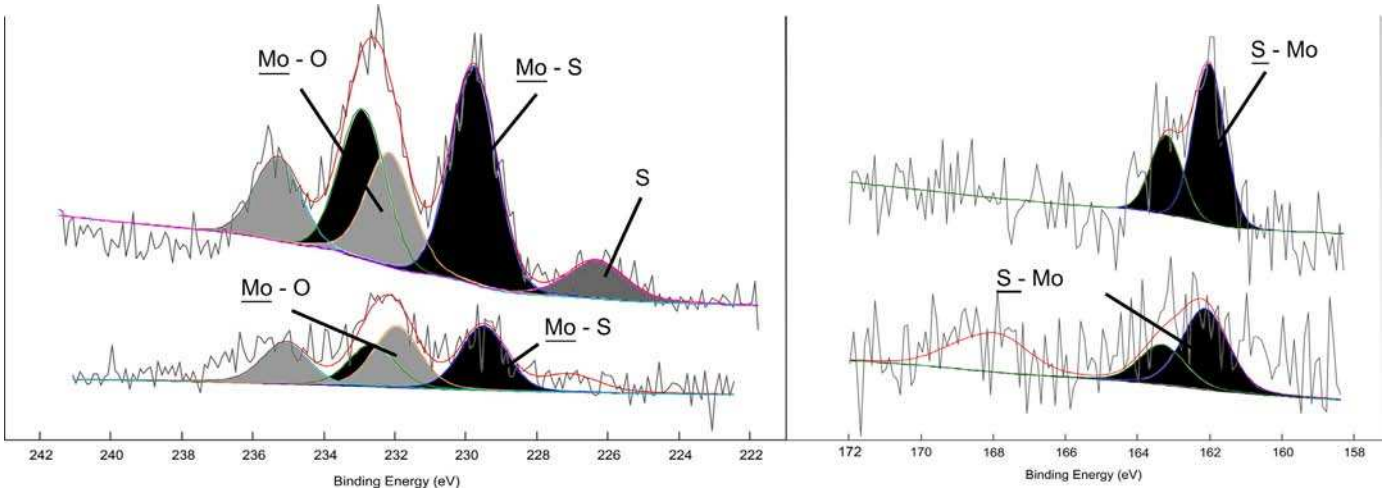

Fig. 14. XPS analyses of the wear scars after 17 min (top spectra) and 4 h (bottom spectra) of testing – Mo 3d (left) and S 2p (right) energy peaks.

starvation of the contact in nanoparticles. The maximum friction reduction achieved during this second hour of the test may have lasted longer than for the reference test with no stirring (36 000 cycles instead of approximately 20 000 cycles) because the contact was well fed in IF-MoS_2 for 72 000 cycles during the first hour, which most likely led to the formation of a thicker and more homogeneous tribofilm. The lubricant was stirred again during the third hour of the test, which led to a significant and immediate reduction of the friction coefficient back to its lowest value of 0.07. Friction then remained low throughout the test, including during

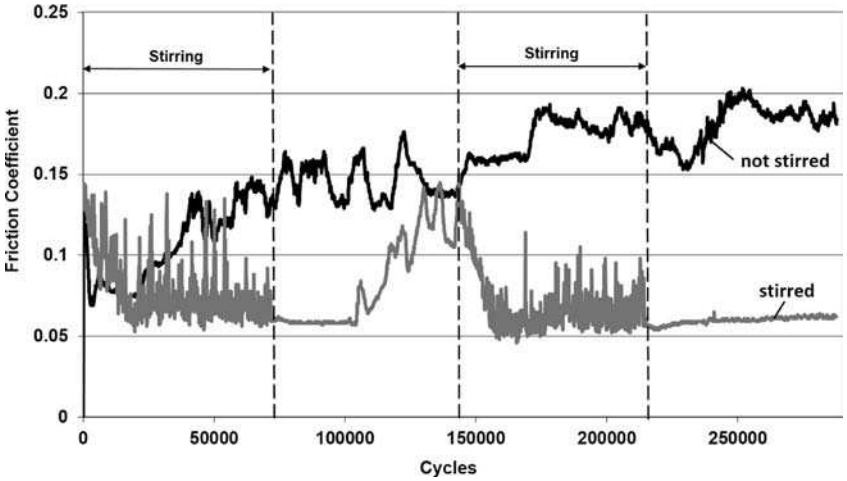

Fig. 15. Performance of LC-type IF-MoS_2 enhanced by modifying the oil flow around the contact.

the fourth hour (cycles 216 000 through 288 000). After 216 000 cycles, the combined two hours of stirring seemingly permitted the formation of a tribofilm thick and homogeneous enough to withstand 72 000 cycles, despite its partial degradation during the second hour of the test.

For the range of MoS_2 nanoparticles studied, these tribological tests show that similar friction coefficients may be obtained regardless of size or crystallinity. In the case where a continuous feeding of the contact in nanoparticles is ensured, for instance through the stirring of the oil, the maximum friction reduction proved stable even for the larger and more crystalline nanoparticles. The inevitable agglomeration of the IF-MoS_2 nanoparticles when no dispersing processes are used (ionic liquids, dispersants…) does not seem to reduce their tribological potential as long as proper oil recirculation is ensured. This observation may be of importance for industrial applications, as fullerene-like nanoparticles have shown significantly reduced capacities when dispersed using classical dispersing agents such as succinimide-base dispersants [23]. The IF-MoS_2 containing more structural defects (either large or small) are however more efficient, as fewer are needed to create and maintain a friction-reducing tribofilm on the contact surfaces. These less crystalline nanoparticles will therefore prove more beneficial in applications where oil recirculation is not ensured such as alternating contacts in finite volumes of oil, or droplet lubrication prior to testing.

3.4. Tribofilm analysis

In order to attribute the differences in nanoparticle performance to their size and morphology alone, the wear surfaces were analyzed by XPS and the compositions of the observed tribofilms were compared to the chemical nature of the IF-MoS_2 recorded previously (Figs. 5 and 6).

The molybdenum (Mo 3d) and sulfur (S 2p) spectra for the poorly crystalline nanoparticles are shown in Fig. 16 (small IF-MoS_2) and Fig. 17 (large IF-MoS_2). At the end of the HFRR tests (Fig. 9), both the Mo $3d_{5/2}$ and the S $2p_{3/2}$ peaks corresponding to MoS_2 (229.8 eV and 162.3 eV for the SpC and 229.9 eV and 162.4 eV for the LpC) can be found on the wear scar, indicating the adhesion of a tribofilm on the wear surfaces. The slight shifting of the S $2p_{3/2}$ peaks toward the lower energies (from 162.7 eV to 162.3 eV) may be due to the presence of iron sulfides. Both surface analyses also revealed peaks corresponding to Mo(VI) and S(VI) species, at 232.7 eV and 169.0 eV in the case of the SpC and 232.5 eV and 168.6 eV for the LpC. These observations are consistent with those made in [17], where two hypotheses are made regarding the adhesion of an MoS_2 tribofilm on a steel substrate. After finding molybdenum and sulfur oxidized species and iron sulfide on a worn surface after IF-MoS_2 testing, the authors evoked the possibilities of either (a) a tribofilm adhesion through the bonding of molybdenum and sulfur with the oxygen found in the native surface oxide layer of the steel, or (b) a quasi-immediate wearing off of the oxide layer at the beginning of the test, followed by S–Fe interactions and oxidization of the tribofilm after its adhesion. A quantification of Fe, Mo and S on the surface revealed an atomic ratio (Fe)/(Fe+Mo+S) of 15% and 17% for the SpC and LpC nanoparticles, respectively, confirming the possible presence of small amounts of iron sulfides in the tribofilm. In the case of the poorly crystalline LpC and SpC IF-MoS_2, the low friction at the end of the tribological tests suggests that the tribofilms found on the wear scar surfaces remain relatively thick and homogeneous, which is consistent with the high concentrations of molybdenum and sulfur (when compared to iron) found on the surface.

The molybdenum (Mo 3d) and sulfur (S 2p) spectra for the more crystalline SC and LC nanoparticles are shown in Figs. 18 and 19, respectively. The analysis carried out on the wear scars after HFRR testing revealed low intensities for the molybdenum and sulfur energy peaks. The atomic ratio (Fe)/(Fe+Mo+S) for these analyses were 44% (SC) and 35% (LC), which confirms that a smaller amount of MoS_2 was found on the worn surface. This is consistent with the results shown in Fig. 9, where the friction coefficient for these more crystalline nanoparticles had increased drastically before the end of the test. The composition of the tribofilm was however similar to those formed when using the poorly crystalline nanoparticles, with the main Mo $3d_{5/2}$ and S $2p_{3/2}$ energy peaks corresponding to the Mo–S species found at 229.5 eV and 161.8 eV for the SC IF-MoS_2 (Fig. 18(b)) and 229.5 eV and 162.1 eV for the LC IF-MoS_2 (Fig. 19(b)). The Mo–O and S–O species observed previously were visible again, with energy peaks found at 232.1 eV and 166.8 eV (small IF-MoS_2, Fig. 18(b)) on the one hand, and 231.9 eV and 167.7 eV (large IF-MoS_2, Fig. 19(b)) on the other.

A more important shifting of the main sulfur energy peaks towards the lower bonding energies (from 162.8 eV to 161.8 eV for the SC IF-MoS_2 and from 162.7 eV to 162.1 eV for the LC IF-MoS_2) was observed for these more crystalline nanoparticles. The higher concentration of iron found on these surfaces may therefore be due to higher quantities of iron sulfides in the tribofilm, altering its lubricating properties. As more wear took place during the testing of the SC and LC IF-MoS_2, these Fe–S species may be due to embedding of wear particles in the tribofilm [24]. These iron sulfides could also have been formed from the interactions

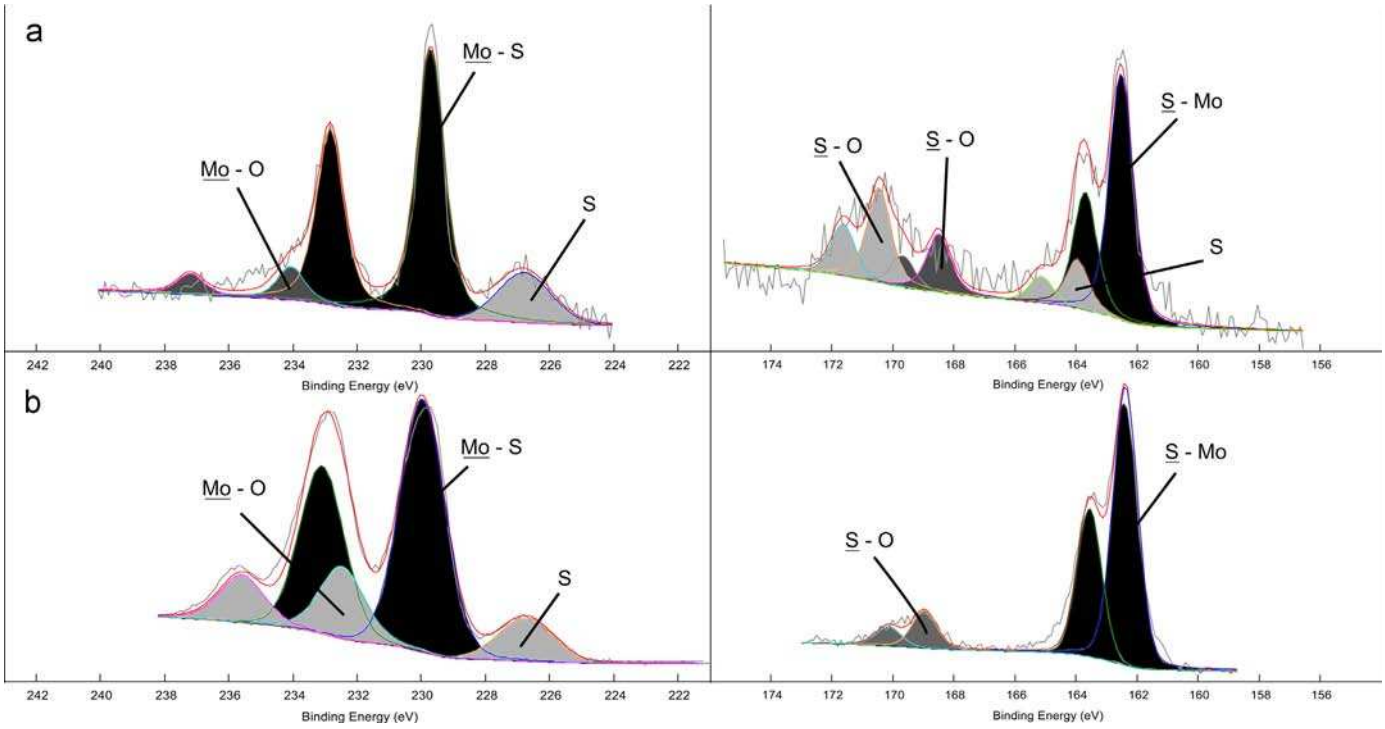

Fig. 16. XPS spectra of molybdenum (left) and sulfur (right) for the SpC IF-MoS_2 (a) powder and (b) tribofilm after 144 000 cycles.

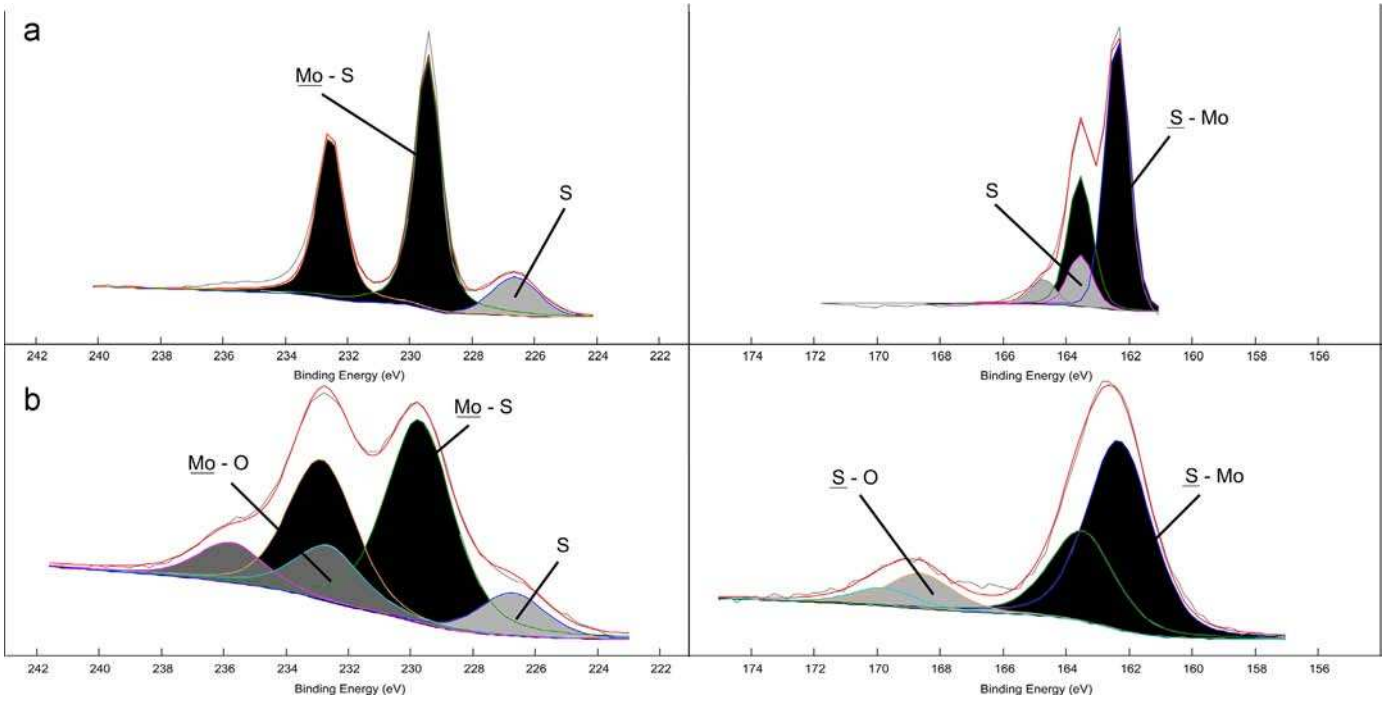

Fig. 17. XPS spectra of molybdenum (left) and sulfur (right) for the LpC IF-MoS_2 (a) powder and (b) tribofilm after 144 000 cycles.

between the sulfur contained in the exfoliated MoS_2 sheets and the Fe atoms of the substrate, enabling the adhesion of the tribofilm. A progressive wearing off of the tribofilm during the HFRR tests would explain why more iron sulfide can be observed for the SC and LC nanoparticles. The fact that iron sulfide was only found at the surface when part of the tribofilm has been worn off would suggest that it may be – at least partly – responsible for the adhesion of the MoS_2 tribofilm on the steel substrate. It remains to be determined whether the Mo–O and S–O bonding by the oxidized species is essential to the adhesion of the tribofilm, or if the oxidization of the MoS_2 tribofilm occurs after its adhesion to the surface. This adhesion does not seem to depend on the initial oxidation level of the IF-MoS_2 nanoparticles, as similar tribofilms were formed after using either small, oxidized, poorly crystalline

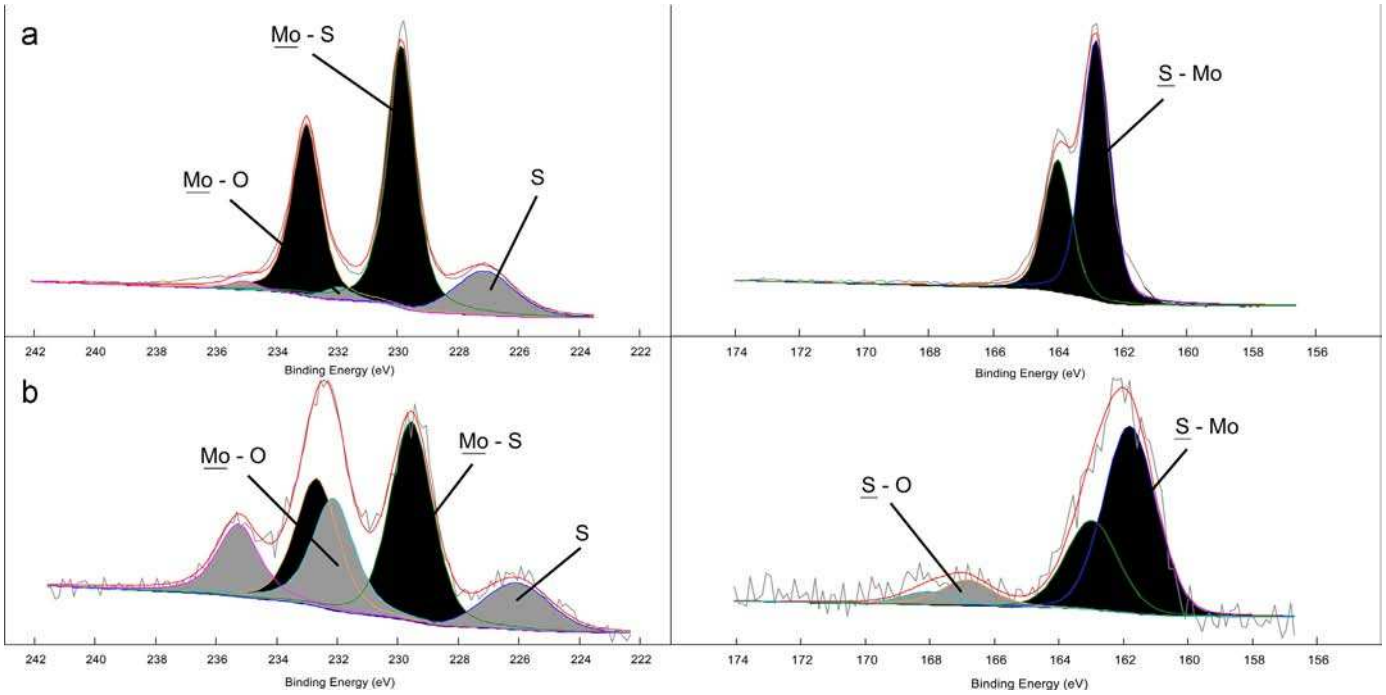

Fig. 18. XPS spectra of molybdenum (left) and sulfur (right) for the SC IF-MoS_2 (a) powder and (b) tribofilm after 144 000 cycles.

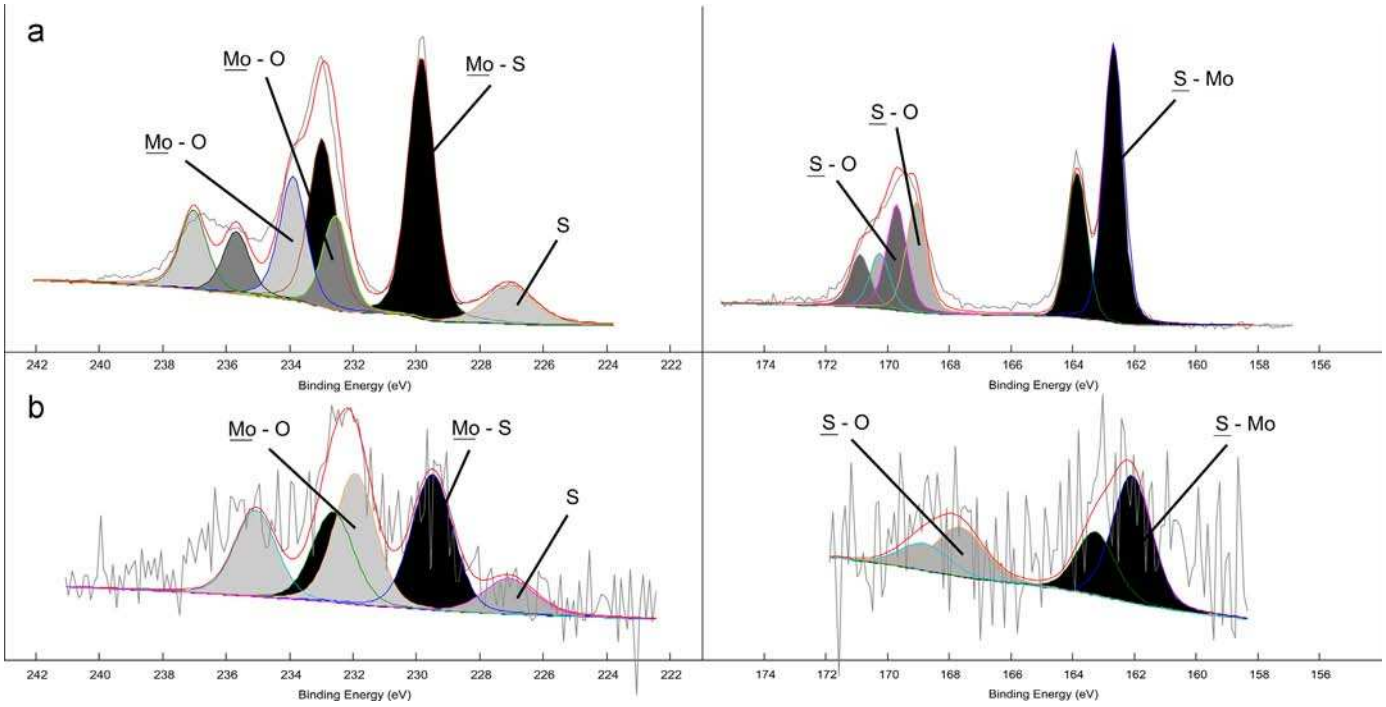

Fig. 19. XPS spectra of molybdenum (left) and sulfur (right) for the LC IF-MoS_2 (a) powder and (b) tribofilm after 144 000 cycles.

IF-MoS_2; small, poorly oxidized, crystalline IF-MoS_2; large, poorly oxidized, poorly crystalline IF-MoS_2; or large, oxidized, crystalline IF-MoS_2.

In order to investigate the degradation of the tribofilm leading to the increase in friction observed at the end of the HFRR tests in the case of the more crystalline nanoparticles, cross sections were extracted from the wear scars resulting from the testing of the SpC and LC IF-MoS_2. The cross sections were taken from the center of the wear scars using the Focused Ion Beam (FIB) technique. The resulting lamellas showed a 10 μm wide area of the extreme surface of the scars.

TEM images of the cross section of the wear scar obtained for the more efficient SpC nanoparticles are shown in Fig. 20. The lamella was covered with a thin platinum layer and a thicker tungsten carbide layer to protect the surface (WC and Pt layers shown in Fig. 20(a)). The tribofilm was found to cover the whole surface of the cross section, with a thickness varying between 30 and 100 nm (Fig. 20(b)). The extreme surface of the tribofilm

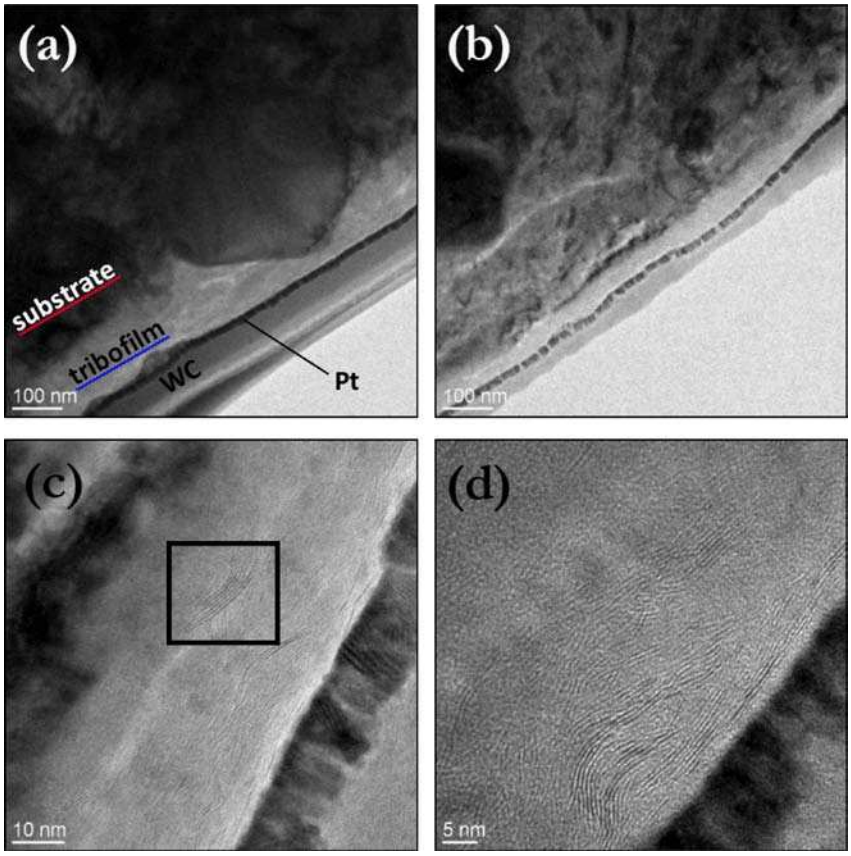

Fig. 20. FIB cross section of the wear scar at the end of the HFRR test for the PAO + 1% SpC IF-MoS_2 blend.

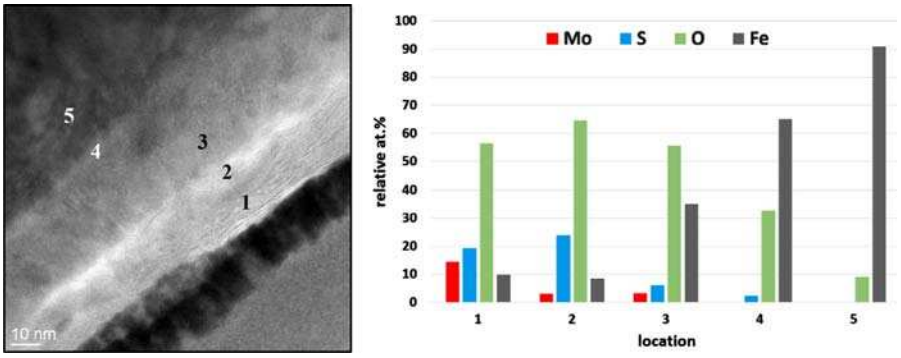

Fig. 21. EDX analyses at different locations inside the tribofilm formed by the SpC IF-MoS_2.

exhibited large layers of MoS_2 platelets, arranged parallel to the surface (Fig. 20(d)). These layers were significantly longer than the MoS_2 platelets found in the nanoparticle structure (Fig. 4(b)), implying that the MoS_2 liberated during the exfoliation of the nanoparticles was rearranged due to the shear in the contact to form these parallel layers. This rearrangement explains the good friction reducing properties of the MoS_2 tribofilm, as the friction between the two original steel counterparts evolves into friction between parallel MoS_2 layers, which exhibit low resistance to shear [25]. Some layers of MoS_2 however seem to have been trapped in the tribofilm without having suffered modifications after their exfoliation from their nanoparticles, as pointed out in Fig. 20(c). These unscathed layers were always found at some distance from the extreme surface, implying that the shear occurring in the contact is responsible for orienting the layers parallel to the surface.

At high magnifications, the tribofilm was often found to be composed of two layers. The top layer, nearest to the surface, appeared close to white on the TEM images and consisted of what resembled parallel MoS_2 platelets. Between this top layer and the substrate was a darker intermediate layer, which did not contain any platelets. Energy-dispersive X-ray spectroscopy (EDX) was carried out on the FIB cross section to obtain the composition of the tribofilm. The numbers in Fig. 21 indicate the locations of the different analyses, and the relative atomic concentrations of molybdenum, sulfur, oxygen and iron are reported on the adjacent graph for each analysis.

Locations 1 and 2 were chosen inside the top layer. The corresponding analyses revealed high contents of molybdenum, sulfur and oxygen and fairly low amounts of iron. This composition is consistent with the XPS analysis showed in Fig. 16, where the top layer of the tribofilm consisted mostly of MoS_2 as well as M–O and S–O species.

The intermediate layer described previously was also analyzed (locations 3 and 4), and revealed much higher concentrations of iron, although molybdenum and sulfur were still found in small quantities. This layer may therefore still contain MoS_2, but is most likely composed of iron oxides and possibly iron sulfides. Its presence may result from the modification of the native iron oxide layer by the bonding of the MoS_2 (through S–Fe and Mo–O species, as suggested in [17]). The native iron oxide layer could also have been partly worn off during the first cycles of the friction test, and this intermediate layer could then result from a bonding of the sulfur found in the MoS_2 platelets with the iron of the substrate. The presence of large quantities of oxygen would then result from the oxidation of the tribofilm during its formation. The composition found at location 4, which was in the intermediate layer but close to the steel substrate, could reinforce this hypothesis. Sulfur was indeed detected but not molybdenum, possibly indicating the presence of iron sulfides which could have enabled the adhesion of the tribofilm. The low amount of sulfur found could however also indicate that molybdenum was also present, but in quantities too low to be detected by the EDX analysis.

The FIB cross section of the wear scar for the more crystalline LC nanoparticles revealed a totally different morphology of the surface, as shown in Fig. 22. Large sections of the cross section were not at all covered by a tribofilm, leaving the bare substrate reach the surface. Other parts of the lamella, on the other hand, contained large areas resembling the intermediate layer of the tribofilm observed previously (Fig. 21). No MoS_2 platelets (such as the ones shown in Fig. 20(d)) were found throughout the entire cross section.

The film was furthermore sometimes found to be trapped inside the substrate, such as shown in Fig. 22(b). Several EDX analyses were carried on this image in order to verify the composition of the different areas. The darker areas (locations 1, 3 and 5) consisted mostly of steel, with very high contents of iron. Traces of molybdenum (location 1) and sulfur (locations 1 and 3) were also found, attesting of a reaction with the MoS_2 from the nanoparticles. Locations 2 and 4 were chosen inside the lighter areas, which appeared to be mostly iron oxides. Low contents of molybdenum and sulfur were also found, with a stoichiometry close to MoS_2. These compositions were similar to the one found on location 3 (Fig. 21), which was in the intermediate layer of the tribofilm.

To confirm that molybdenum and sulfur were found below the surface of the wear scar, an EDX maps tracing Mo, S, Fe, O and Pt was carried out on the FIB cross section (Fig. 23). The edge of the sample is made visible by the platinum layer, and the substrate is recognized by the high concentrations of iron. These images clearly reveal areas containing large amounts of molybdenum, sulfur and oxygen trapped inside the steel substrate.

The absence of a tribofilm on large portions of the extreme surface, as well as the change in composition of the tribofilm in the remaining areas (with the absence of MoS_2 platelets), explains the much higher friction coefficient recorded at the end of the HFRR test for the LC IF-MoS_2 compared to the SpC nanoparticles. These TEM observations also provide indications regarding the evolution of the tribofilm in the case of the more crystalline nanoparticles. The surface was indeed likely to resemble the one observed for the SpC IF-MoS_2 during the beginning of the test, when maximum friction reduction was achieved (cycles 10 000 to 90 000 in Fig. 9). The sufficient amount of LC nanoparticles then entering the contact ensured the formation of an efficient MoS_2 tribofilm, with MoS_2 layers aligned parallel to the surface providing great friction and wear reduction. The progressive starvation of the contact in IF-MoS_2, combined to the lower exfoliating

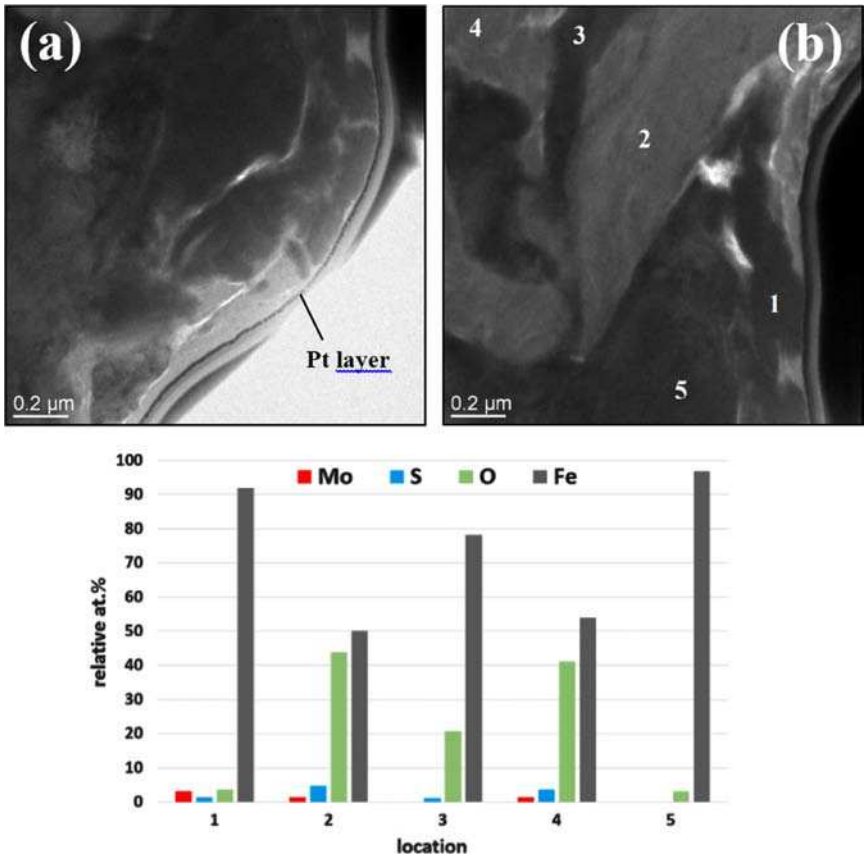

Fig. 22. FIB cross section of the wear scar at the end of the HFRR test for the PAO+1% LC IF-MoS2 blend.

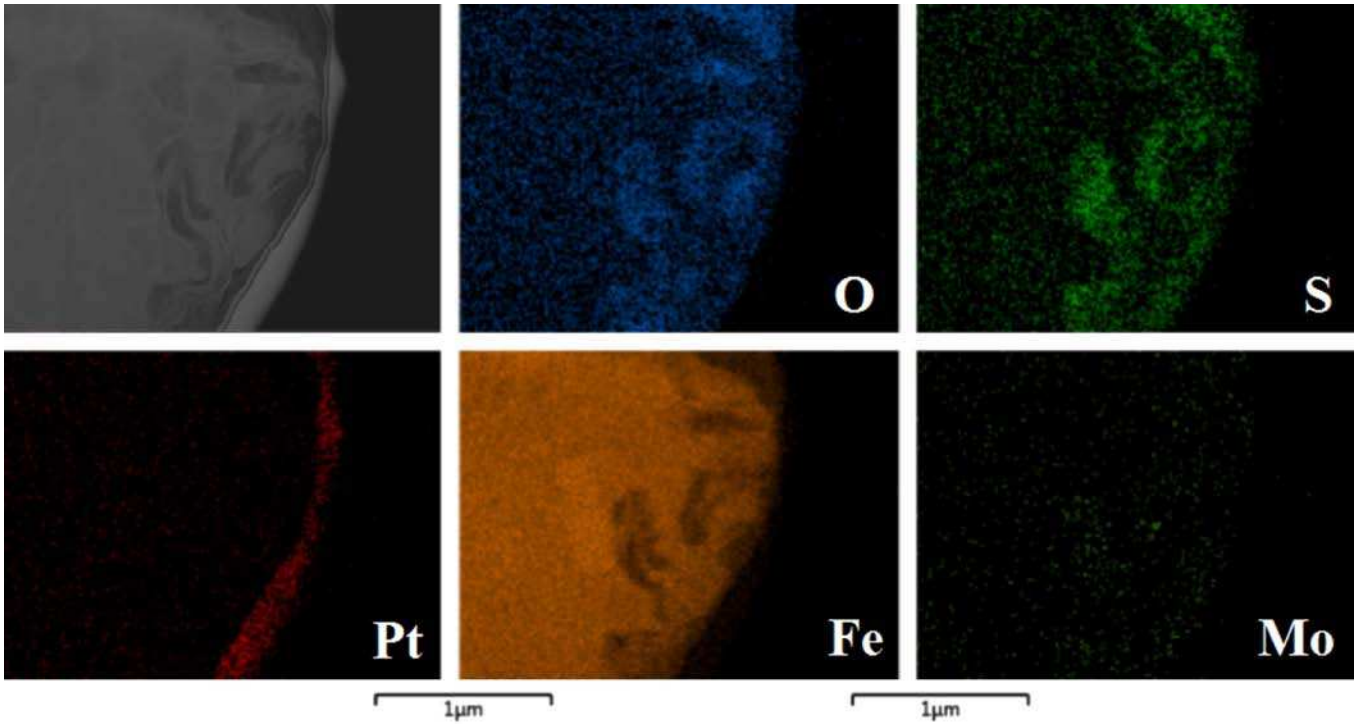

Fig. 23. EDX mapping of the main elements present on the FIB cross section of the wear scar for the LC IF-MoS_2.

capacities of the more crystalline nanoparticles, then led to fewer MoS_2 platelets reaching the contact surfaces. As the regeneration of the tribofilm was slowed down, the continued rubbing of the surfaces most likely caused a progressive wear of the top layer of the tribofilm (locations 1 and 2 in Fig. 21). As the tribofilm formed was not homogeneous and of equal initial thickness throughout the surface, this wearing off led to steel–steel contacts in some places while others were still covered by a tribofilm with a composition similar to that of the intermediate layer observed in Fig. 21 (locations 3 and 4). The increasing number of steel–steel contacts would then lead to a progressive rise in friction and wear as adhesion (through localized micro-welding) would be likely to take place. This could in turn lead to the covering of the remaining tribofilm by steel through the smearing of the surface, which would explain why traces of sulfur and molybdenum were found as deep as 1 μm beneath the extreme surface at the end of the test with the LC nanoparticles.

3.5. *Tribological properties of commercial h-MoS_2*

The results shown in this study indicate that the main parameter governing IF-MoS_2 efficiency is their crystallinity, regardless of size. The IF-MoS_2 generating the most friction reduction were the SpC and LpC nanoparticles, which did not have a "fullerene-like" aspect due to their many structural defects. In the light of these results, the use of perfectly engineered fullerene-like nanoparticles seems questionable. A recent study by Kogovsek et al. [26] furthermore suggests that the chemical nature of the additives affects friction reduction much more significantly than their size or shape, as similar tribological test results were obtained for many different kinds of MoS_2 micro- and nanoparticles (nanotubes, 2 μm platelets and 10 μm platelets). To verify these hypotheses, the tribological performances of bulk MoS_2 particles were compared to those of the poorly crystalline IF-MoS_2 tested before. These particles consisted in micrometric assemblies of MoS_2 platelets (Fig. 24). An XPS analysis was carried out on the MoS_2 powder (Fig. 25), revealing their purity. The h-MoS_2 was added to the PAO base oil tested previously, with a weight concentration of 1%. The operating conditions used were the same as those described in Fig. 1.

The h-MoS_2 proved much less effective than the IF-MoS_2 nanoparticles in boundary lubrication, with a minimum coefficient of friction achieved of 0.09 instead of 0.06 (Fig. 26). These particles were also less efficient in time, as the maximum friction reduction only lasted for a few cycles before friction started increasing back to the value achieved with the base oil alone. The IF-MoS_2 were also more effective in reducing wear, as the corresponding wear scars were significantly smaller than the one obtained when using the h-MoS_2 (Fig. 27).

This final test confirmed the interest in using nano-sized nanoparticles for reducing friction and wear in severe boundary lubrication regimes. For equal weight concentrations, the availability of these bigger microparticles in and near the contact is thought to be too low to ensure permanent tribofilm regeneration. Nanoparticles may also pass through the contact more easily because of their reduced size. For real-life applications, the use of IF-MoS_2 nanoparticles over MoS_2 microparticles furthermore holds many more advantages: their low mass and small size should facilitate their dispersion in the oil media and reduce the risks related to clogging, and their spherical and closed structure are more likely to reduce chemical interactions with other additives or surfaces outside the contact area.

4. Conclusions

1. Four types of IF-MoS_2 of different sizes and morphologies were tested in severe conditions under pure sliding (boundary lubrication regime, splash lubrication with 2 mL of oil and high number of cycles). All IF-MoS_2 proved very effective in reducing friction and wear, with the most efficient nanoparticles maintaining maximum friction reduction (from 0.20 to 0.06) for more than 120 000 cycles.

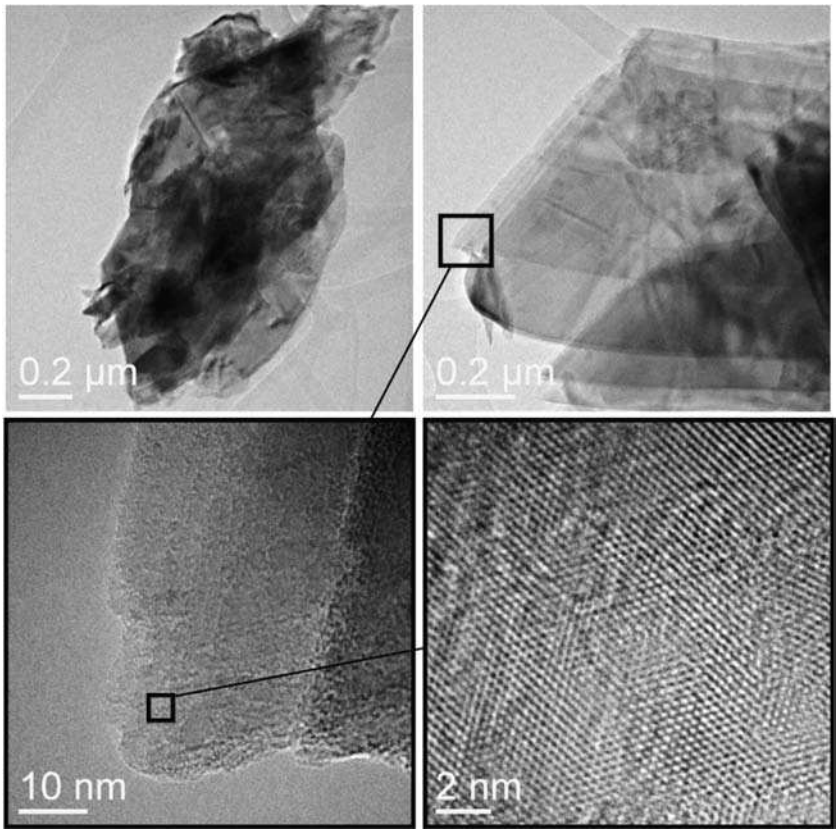

Fig. 24. HR-TEM images of the bulk MoS_2 particles revealing their hexagonal atomic structure.

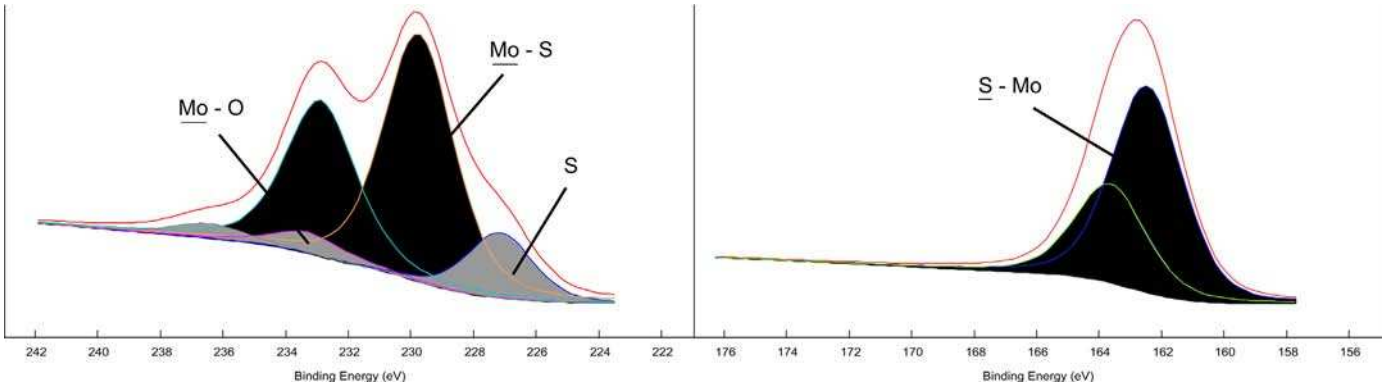

Fig. 25. XPS spectra of molybdenum (right) and sulfur (left) of the bulk MoS_2 particles.

2. In the conditions studied, nanoparticle size and morphology did not impact the minimum friction coefficient reached. The presence of structural defects in the nanoparticles did however affect their effectiveness in time, as the poorly crystalline IF-MoS_2 (not "fullerene-like") maintained minimum friction over a significantly higher number of cycles, regardless of their size. The facilitated exfoliation of these nanoparticles under the combined actions of normal pressure and shear is thought to facilitate tribofilm formation and regeneration when a fewer number of nanoparticles is available in the contact.
3. The efficiency of the more crystalline fullerene-like nanoparticles in time was found to match that of the less crystalline IF-MoS_2, as long as proper oil recirculation is ensured during the test. The deterioration of the tribofilm after a given number of cycles is thought to be due to a progressive starvation of the contact in nanoparticles, which can be avoided by maintaining a homogeneous dispersion of the IF-MoS_2 in the oil. This may be achieved by mixing the oil, or by using adequate dispersants.
4. XPS analyses were carried out on all the IF-MoS_2 powders and on the wear scars after tribological testing. Although some nanoparticles seemed more oxidized than others, this did not seem to affect the tribochemistry of the contact as all the tribofilms formed on the surfaces had similar chemical compositions. In the case of the more crystalline nanoparticles, the higher atomic concentration of iron relative to Mo and S and the bigger shifting of the sulfur peaks toward lower energies suggested higher quantities of iron sulfides on the wear surfaces. The observation of FIB cross sections of the wear surfaces for both the poorly crystalline and the more crystalline nanoparticles revealed the evolution of the surface during the HFRR tests. A 50–100 nm tribofilm first forms on the surface, consisting of two main layers. The top, thinner layer is made of

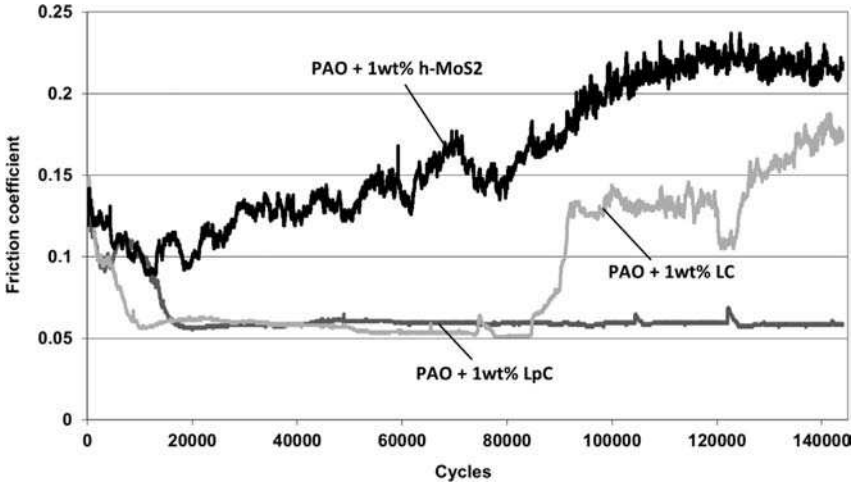

Fig. 26. Comparison of the friction reducing properties of h-MoS2 particles and IF-MoS2 nanoparticles.

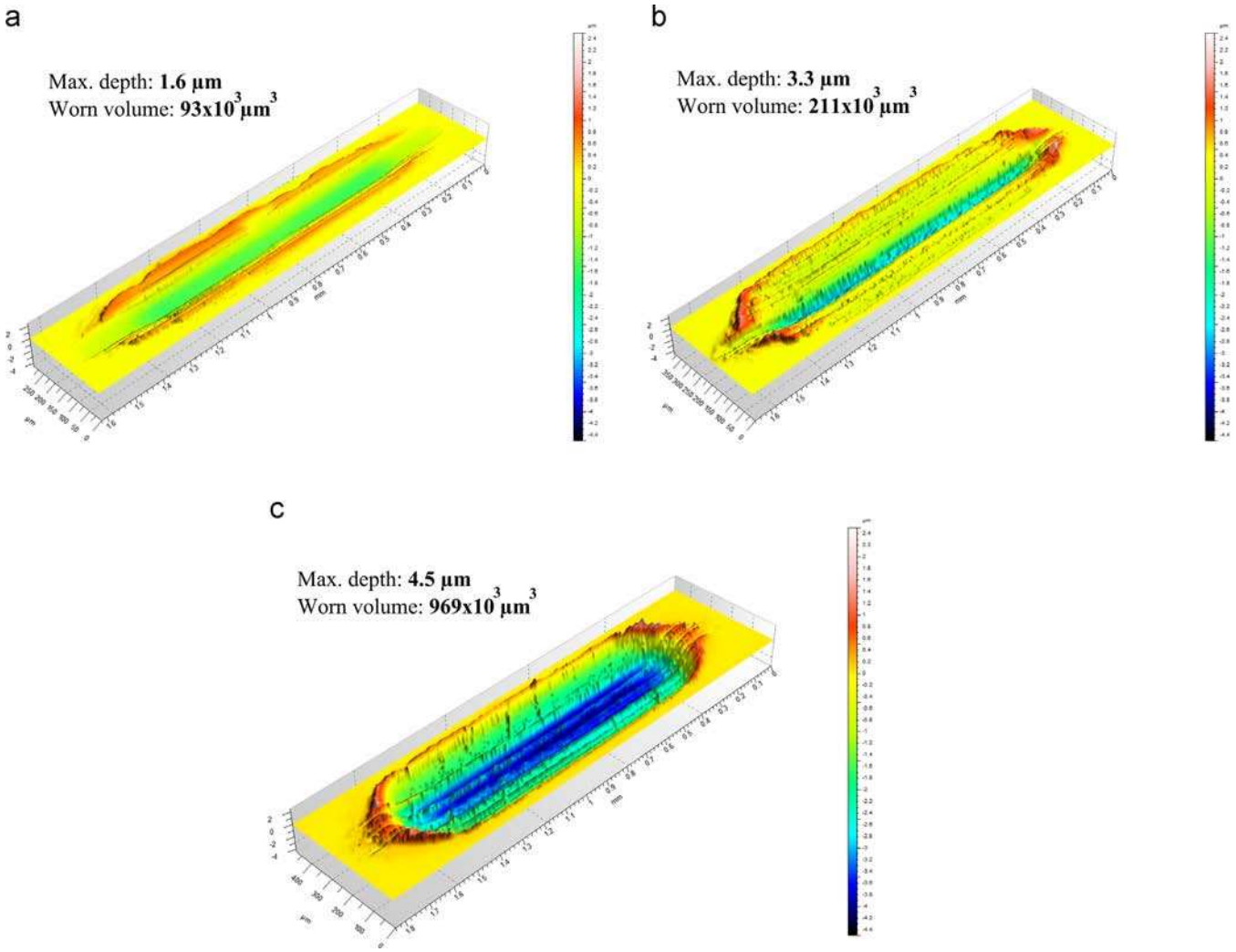

Fig. 27. Wear scars after the HFRR testing of (a) LpC IF-MoS_2, (b) LC IF-MoS_2, and (c) h-MoS_2.

MoS_2 platelets arranged parallel to the surface, providing low friction in the contact. An intermediate layer, containing iron oxides and sulfides, links it to the substrate. In the case of the more crystalline IF-MoS_2, their difficulty to exfoliate combined to the starvation of the contact in nanoparticles leads to a progressive wearing off of the tribofilm and to the apparition of steel–steel contacts, increasing the friction and wear in the contact.

5. As size did not affect nanoparticle efficiency for a given morphology (for diameters ranging from 150 nm to 350 nm and in the test conditions used), the tribological performance of bulk MoS_2 microparticles were compared to those of the

IF-MoS_2. This test confirmed the interest of using nano-sized particles, as the MoS_2 microparticles produced higher friction and wear than the IF-MoS_2. The poorer availability of these significantly bigger particles in and around the contact (for a given weight concentration) is thought to be responsible for their lower performances.

Acknowledgments

The authors would like to express their gratitude to the CLYM (Centre LYonnais de Microscopie) and to Christophe Géantet from IRCELYON (Institut de Recherches sur la Catalyse et l'Environnement de Lyon) for their precious help, to LUBRIZOL for providing the base oil used in this study, as well as to the ANRT (Association Nationale de la Recherche et de la Technologie) for their support.

References

[1] R. Tenne, Advances in the synthesis of inorganic nanotubes and fullerene-like nanoparticles, Angew. Chem. Int. Ed. 42 (2003) 5124–5132.
[2] V.N. Bakunin, A.Y.u. Suslov, G.N. Kuzmina, O.P. Parenago, Synthesis and application of inorganic nanoparticles as lubricant components – a review, J. Nanopartic. Res. 6 (2004) 273–284.
[3] M. Bar-Sadan, I. Kaplan-Ashiri, R. Tenne, Inorganic fullerenes and nanotubes: wealth of materials and morphologies, Eur. Phys. J. Spec. Top. 149 (2007) 71–101.
[4] L. Joly-Pottuz, N. Matsumoto, H. Kinoshita, B. Vacher, M. Belin, G. Montagnac, J.M. Martin, N. Ohmae, Diamond-derived carbon onions as lubricant additives, Tribol. Int. 41 (2008) 69–78.
[5] D.-L. Cursaru, C. Andrinescu, C. Pirvu, R. Ripeanu, The efficiency of Co-based single wall carbon nanotubes (SWNTs) in comparison with a commercial additive as AW and EP additives to mineral base oil, Wear 290–291 (2012) 133–139.
[6] F. Dassenoy, L. Joly-Pottuz, J.-M. Martin, D. Vrbanic, A. Mrzel, D. Mihailovic, W. Vogel, G. Montagnac, Tribological performances of $Mo_6S_3I_6$ nanowires, J. Eu. Ceram. Soc. 27 (2007) 915–919.
[7] J. Padgurskas, R. Rukuiza, I. Prosycevas, R. Kreivaitis, Tribological properties of lubricant additives of Fe, Cu and Co nanoparticles, Tribol. Int. 60 (2013) 224–232.
[8] L. Cizaire, B. Vacher, T. Le Mogne, J.M. Martin, L. Rapoport, A. Margolin, R. Tenne, Mechanisms of ultra-low friction by hollow inorganic fullerene-like MoS_2 nanoparticles, Surf. Coat. Tech. 160 (2002) 282–287.
[9] L. Joly-Pottuz, F. Dassenoy, M. Belin, B. Vacher, J.-M. Martin, N. Fleischer, Ultralow-friction and wear properties of IF-WS_2 under boundary lubrication, Tribol. Lett. 18 (4) (2005) 477–485.
[10] R. Rosentsveig, A. Gorodnev, N. Feuerstein, H. Friedman, A. Zak, N. Fleischer, J. Tannous, F. Dassenoy, R. Tenne, Fullerene-like MoS_2 nanoparticles and their tribological behavior, Tribol. Lett. 36 (2009) 175–182.
[11] J. Tannous, F. Dassenoy, A. Bruhacs, W. Tremel, Synthesis and tribological performance of novel $Mo_xW_{1-x}S_2$ ($0 \le x \le 1$) inorganic fullerenes, Tribol. Lett. 37 (2010) 83–92.
[12] L. Joly-Pottuz, J.M. Martin, F. Dassenoy, M. Belin, G. Montagnac, B. Reynard, N. Fleischer, Pressure-induced exfoliation of inorganic fullerene-like WS_2 particles in a Hertzian contact, J. Appl. Phy. 99 (2006) 023524.
[13] I. Lahouij, F. Dassenoy, L. de Knoop, J.-M. Martin, B. Vacher, In situ TEM observation of the behavior of an individual fullerene-like MoS_2 nanoparticle in a dynamic contact, Tribol. Lett. 42 (2011) 133–140.
[14] I. Lahouij, F. Dassenoy, B. Vacher, J.-M. Martin, Real time TEM imaging of compression and shear of single fellerene-like MoS_2 nanoparticle, Tribol. Lett. 45 (2012) 131–141.
[15] O. Tevet, O. Goldbart, S.R. Cohen, R. Rosentsveig, R. Popovitz-Biro, H.D. Wagner, R. Tenne, Nanocompression of individual multilayered polyhedral nanoparticles, Nanotechnology 21 (2010) 365705.
[16] O. Tevet, P. Von-Huth, R. Popovitz-Biro, R. Rosentsveig, H. Daniel Wagner, R. Tenne, Friction mechanism of individual multilayered nanoparticles, PNAS 108 (50) (2011) 19901–19906.
[17] J. Tannous, F. Dassenoy, I. Lahouij, T. Le Mogne, B. Vacher, A. Bruhacs, W. Tremel, Understanding the tribochemical mechanisms of IF-MoS_2 nanoparticles under boundary lubrication, Tribol. Lett. 41 (2011) 55–64.
[18] I. Lahouij, B. Vacher, J.-M. Martin, F. Dassenoy, IF-MoS_2 based lubricants: influence of size, shape and crystal structure, Wear 296 (2012) 558–567.
[19] A. Moshkovith, V. Perfiliev, I. Lapsker, N. Fleischer, R. Tenne, L. Rapoport, Friction of fullerene-like WS_2 nanoparticles: effect of agglomeration, Tribol. Lett. 24 (3) (2006) 225–228.
[20] A. Moshkovith, V. Perfiliev, A. Verdyan, I. Lapsker, R. Popovitz-Biro, R. Tenne, L. Rapoport, Sedimentation of IF-WS_2 aggregates and a reproductibility of the tribological data, Tribol. Int. 40 (2007) 117–124.
[21] S. Aralihalli, S.K. Biswas, Grafting of dispersants on MoS_2 nanoparticles in base oil lubrication of steel, Tribol. Lett. 49 (2013) 61–76.
[22] P. Afanasiev, I. Bezverkhy, Synthesis of MoS_x ($5 > x > 6$) amorphous sulfides and their use for preparation of MoS_2 monodispersed microspheres, Chem. Mater 14 (2002) 2826–2830.
[23] P. Rabaso, F. Dassenoy, F. Ville, M. Diaby, B. Vacher, T. Le Mogne, M. Belin, J. Cavoret, An investigation on the reduced ability of IF-MoS_2 nanoparticles to reduce friction and wear in the presence of dispersants, Tribol. Lett. 55 (2014) 503–516.
[24] P. Njiwa, A. Hadj-Aïssa, P. Afanasiev, C. Geantet, F. Bosselet, B. Vacher, M. Belin, T. Le Mogne, F. Dassenoy, Tribological properties of new MoS_2 nanoparticles prepared by seed-assisted solution technique, Tribol. Lett. 55 (2014) 473–481.
[25] J.-M. Martin, C. Donnet, T. Le Mogne, Superlubricity of molybdenum disulphide, Tribol. Int. 33 (2) (2000) 148–149.
[26] J. Kogovsek, M. Kalin, Various MoS_2, WS_2, and C-based micro- and nanoparticles in boundary lubrication, Tribol. Lett. 53 (2014) 585–597.